GKSS FORSCHUNGSZENTRUM in der HELMHOLTZ-GEMEINSCHAFT

Hindcast simulation of the North Sea by HAMSOM for the period of 1948 till 2007 – temperature and heat content

Authors:

E. M. I. Meyer
T. Pohlmann
R. Weisse

ISSN 0344-9629

HELMHOLTZ | GEMEINSCHAFT

wissen schafft nutzen

GKSS 2009/3

GKSS 2009/3

Hindcast simulation of the North Sea by HAMSOM for the period of 1948 till 2007 – temperature and heat content

Authors:

E. M. I. Meyer
T. Pohlmann
R. Weisse

(Institute for Coastal Research)

GKSS-Forschungszentrum Geesthacht GmbH · Geesthacht · 2009

Die Berichte der GKSS werden kostenlos abgegeben.
The delivery of the GKSS reports is free of charge.

Anforderungen/Requests:

GKSS-Forschungszentrum Geesthacht GmbH
Bibliothek/Library
Postfach 11 60
21494 Geesthacht
Germany
Fax.: +49 4152 87-17 17

Als Manuskript vervielfältigt.

ISSN 0344-9629

GKSS-Forschungszentrum Geesthacht GmbH · Telefon (04152) 87-0
Max-Planck-Straße 1 · 21502 Geesthacht / Postfach 11 60 · 21494 Geesthacht

GKSS 2009/3

Hindcast simulation of the North Sea by HAMSOM for the period of 1948 till 2007 – temperature and heat content

Elke M. I. Meyer, Thomas Pohlmann and Ralf Weisse

55 pages with 31 figures and 5 tables

Abstract

Long-term changes and variability in water temperature, heat content, and thermocline structure in the North Sea for the period of 1948 to 2007 are investigated by means of a model reconstruction using the baroclinic shelf sea model HAMSOM. The model was driven by observed (reanalysed) atmospheric conditions obtained from the NCEP/NCAR global reanalysis. It was found that HAMSOM reasonably well reproduced observed trends and variabilities on time scales from years to decades. In particular, a strong increase in North Sea temperatures and heat content after the early 1980s was obtained which is in good agreement with that obtained from long-term sea surface temperature (SST) records observed in the area. A number of sensitivity experiments were carried out to elaborate on the relative contributions of the various atmospheric forcing parameters on the observed increase in SST. It was found that regional changes in atmosphere-ocean heat exchange may account for a considerable fraction of the observed long-term changes and variability.

Rekonstruktion der Temperatur und des Wärmeinhalts der Nordsee für die Periode von 1948 bis 2007 mit Hilfe des regionalen Schelfmeermodells HAMSOM

Zusammenfassung

Die langzeitlichen Änderungen und die Variabilität von Wassertemperatur, Wärmeinhalt und Struktur der Thermokline in der Nordsee sind für den Zeitraum von 1948 bis 2007 untersucht worden. Diese Untersuchungen sind anhand von Rekonstruktionen erfolgt, die mit dem baroklinen Schelfmodell HAMSOM (HAMburg Shelf Ocean Model) gerechnet worden sind. Reanalyse-Daten von NCEP/NCAR, in denen Beobachtungen berücksichtigt sind, wurden für den atmosphärischen Antrieb benutzt. HAMSOM reproduziert im Vergleich zu Messungen die Trends und Variabilitäten auf jährlichen bis dekadischen Zeitskalen qualitativ zufriedenstellend. Insbesondere wurde ein starker Anstieg der Wassertemperatur und des Wärmeinhalts seit den 1980er Jahren von HAMSOM simuliert, der in guter Übereinstimmung mit Beoachtungen ist. In einer Sensitivitätsstudie wurde der Anteil von verschiedenen atmosphärischen Antriebsparametern am beobachteten Anstieg der Wassertemperatur untersucht. Die Experimente zeigen, dass regionale Änderungen im Wärmeaustausch zwischen Ozean und Atmosphäre einen entscheidenden Anteil an den beobachteten langzeitlichen Änderungen haben können.

Manuscript received / Manuskripteingang in TFP: 27. Mai 2009

Contents

1 Introduction

The North Sea represents one of the best sampled and analysed continental shelf seas of the world. A large number of different measurements exists comprising, for example, in-situ data from long-term routine measurement programs (Wiltshire and Manly, 2004; Becker et al., 1997, DOD[1], BODC[2]) or from relatively short but more comprehensive measurement campaigns (Moll and Radach, 1990; Charnock et al., 1994; Howarth et al., 1994). While most of the in-situ data are from relatively near-shore areas or along certain transects, satellite data have become increasingly available in the recent decades and complement existing in-situ measurements, mostly for the more offshore regions. However, satellite data only provide information from variables at the sea surface and there are still considerable gaps for the deeper layers, but also in space and time. Nevertheless climatological data sets of temperature and salinity (interpolated from measurements) have been compiled for the North Sea (Damm, 1989, 1997; Janssen et al., 1999; Janssen, 2002).

When long-term changes and variability over decades of years are considered, homogeneity and consistency of the analysed data sets become a major issue (Karl et al., 1993; von Storch and Weisse, 2008). In particular, changes in the density of observational network, procedures or measurement and analysis techniques over time may introduce spurious signals in the data that do not reflect changes in the variable considered but merely reflect changes in the way the measurements have been taken e.g. Bengtsson et al. (2004). In atmospheric research global reanalysis have become a common tool to reduce such inhomogeneities and to provide a dynamically consistent picture in space and time (e.g. Kalnay et al. (1996); Uppala et al. (2005)). Such reanalysis are now also common to drive regional atmosphere models (Feser et al., 2001; Sotillo et al., 2005), wind wave and sea level models (Weisse and Günther, 2007; Ratsimandresey et al., 2008; Sebastião et al., 2008; Jędrasik et al., 2008; Pilar et al., 2008) or ocean models (Omstedt and Hansson, 2006; Demirov and Pinardi, 2002; Tonani et al., 2008; Gordon and McClean, 1999; O'Driscoll and Kamenkovich, 2009) to obtain a similar consistent pictures for the considered systems. For the North Sea, such efforts have been carried out by e.g. Backhaus and Hainbucher (1987); Schrum et al. (2003); Skogen and Moll (2005); Holt et al. (2005); Pohlmann (2006).

Increasing computing power in the recent years results in the use of increasingly complex quasi-realistic ocean models simulating increasingly longer periods. For the North Sea, today complex mesoscale baroclinic ocean models are in use for such exercises (Holt and James, 2001; Holt et al., 2005; Siddorn et al., 2007; Winther and Evensen, 2006; Burchard and Bolding, 2001; Umlauf and Burchard, 2005; Luyten et al., 2003; Skogen and Søiland, 1998; de Kok et al., 2001; Pohlmann,

2006).

The European model inter-comparison study NOMADS2 compared a number of such quasi-realistic North Sea models and demonstrated that the quality of these models has considerably converged in the last few years although there are still significant differences for some of the variables (Delhez et al., 2004).

In this study, we use the three-dimensional baroclinic shelf sea model HAMSOM [HAMburg Shelf Ocean Model] (Backhaus, 1985; Pohlmann, 1996) driven by the NCEP/NCAR global reanalysis atmospheric forcing (Kalnay et al., 1996) to reconstruct at high spatial ($2.5^\circ \times 2.5^\circ$) and temporal (6 hour) detail the thermodynamic conditions 1948-2007 of the North Sea. To our knowledge, such a simulation presently represents the longest reconstruction of regional conditions in the North Sea. The results are compared with existing measurements and the ability of the simulation to reconstruct observed long-term changes is investigated. Sensitivity experiments are carried out to elaborate on the causes of the observed long-term changes, in particular on the strong increase in temperature and heat content observed since the early 1980s. The manuscript is structured as follows. In chapter 2 the model and model validation are briefly described. Reconstructed changes in temperature, thermocline structure and heat content are discussed in chapters 3, 4 and 5. The sensitivity experiments and their results are presented in chapter 6. Eventually, in chapter 7 our results are summarized and discussed. Additional information to mean temperature and heat content are in Appendix A to C.

[1] DOD - Deutsches Ozeanographisches Datenzentrum (German Oceanographic Data Centre)

[2] BODC - British Oceanographic Data Centre

2 Model and Validation

2.1 Model Description and Set-up

HAMSOM represents a quasi-realistic, three-dimensional baroclinic shelf sea model. For the North Sea, there are more than 20 years experience in using HAMSOM for modelling physical processes and variability (Backhaus and Hainbucher, 1987; Pohlmann, 1996, 2006; Schrum and Backhaus, 1999). In this study, HAMSOM was set up at a spatial resolution of $20' \, x \, 12'$ and 19 vertical levels covering the greater North Sea area (Figure 2.1). Layer thicknesses vary between $5\,m$ in the upper $50\,m$ and $400\,m$ near the bottom at the North Atlantic boundary. A time step of five minutes is applied which is permitted by an implicit formulation of vertical diffusion, vertical shear stress and gravity waves. All others terms are formulated explicitly. At the open boundaries, lateral boundary conditions are obtained from a coarser, large-scale Northwest-European shelf sea model driven by climatological temperature and salinities obtained from Levitus (1982). For water levels, in addition the eight most significant tidal constituents (M_2, S_2, N_2, K_2, K_1, O_1, Q_1, P_1) are included and weather effects are accounted for by using wind and pressure fields from the NCEP/NCAR Reanalysis 1 (Kalnay et al., 1996).

Under inflow conditions temperature and salinity at the lateral boundaries are obtained from the Northwest European Shelf Sea model, while the Sommerfeld radiation condition is applied for outflow conditions (Orlanski, 1976). Climatological monthly mean river run-off from the most important sources is included (Damm, 1997). At the bottom a quadratic stress law is applied. A set of parameterisations providing the most reasonable results for the North Sea (Pohlmann, 2006) was used. In particular, at the sea surface fluxes of momentum, heat and fresh water were calculated from meteorological parameters (near-surface marine wind speed, sea surface pressure, air temperature at $2\,m$ height, sea surface temperature, relative humidity, total cloud cover and total precipitation) using bulk formulae. The parameterisation for incoming solar radiation was taken from the COHERENS model (Luyten et al., 1999), while the outgoing long-wave radiation was calculated according to Fung et al. (1984). For sensible and latent heat flux the parameterisations from Kondo (1975) were used.

Atmospheric forcing was obtained from the NCEP/NCAR reanalysis 1 data set (Kalnay et al., 1996) comprising near-surface air temperature, humidity, cloud cover, precipitation, sea level pressure and near-surface wind speed and direction. Siegismund and Schrum (2001) showed that the main features of the large-scale atmospheric circulation over the North Sea are represented reasonably well by the NCEP/NCAR reanalysis. Full model output has been stored every hour comprising three-

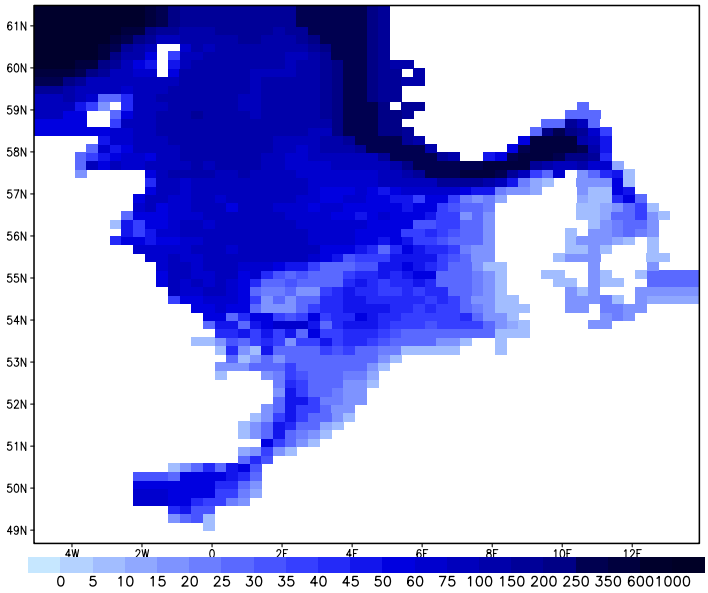

Figure 2.1: *Model domain and bathymetry of HAMSOM [m].*

dimensional fields of temperature, salinity, and horizontal velocity components as well as 2d water level elevations.

2.2 Validation of Model Results

Extensive validation of the HAMSOM model in the present set-up has been provided by Pohlmann (1996) and Pohlmann (2006) who compared the model with data from the FLEX'76 experiment and with measurements collected at the DOD. In the following, some additional validation is performed using SST data from Helgoland Roads (Wiltshire and Manly, 2004; Franke et al., 2004) and SST data from three light vessels in the German Bight (DOD).

In Table (2.1) the results of the comparison are shown. Correlations vary between 0.83 and 0.89. Bias and root-mean-square-error between observations and simulation range from 0.31 K to 0.66 K and from 0.82 K to 1.20 K, respectively. Table (2.2) shows the number of observations per month entering the analysis. It can be inferred that for the light vessels Elbe I and P11/P8 the error statistics are representative for annual mean conditions. For Helgoland roads and P15/P12, more data were available in summer/winter and the statistics are more representative for the respective seasons.
As we are more interested in the simulation of long-term variability and change some more specific comparison for Helgoland has been made. Helgoland is the central island in the German Bight, about 60 km offshore and can be considered as representative for the south eastern part of the model domain. The observations from Helgoland constitute a very long record starting in 1873 until today, but it includes some longer gaps (Wiltshire and Manly, 2004; Franke et al., 2004, DOD). To concentrate on longer time scales, 5-year running means of observed and simulated SST at

	Time	Latitude	Longitude	Number of data	Correlation	Bias [K]	RMSE [K]
Helgoland	2.1.1962–28.12.2007	54.18°	7.9°	11464	0.89	0.60	1.12
Elbe I	1.1.1950–22.4.1988	54.00°	8.18° / 8.12°	13852	0.83	0.66	1.20
P11/P8	1.1.1950–11.3.1978	54.27°	7.2°	1014	0.84	0.31	0.82
P15/P12	1.1.1950–21.5.1986	54.00° /54.18°	7.85° / 7.45°	8166	0.83	0.37	0.95

Table 2.1: *Validation statistic for SST at Helogland Roads and three light vessels (Elbe I, P11/P8 and P15/P12) in the German Bight. The periods for which the comparisons have been made is indicated in the column* time*. The statistics (correlation, bias, and root-mean-square error [RMSE]) have been obtained from daily data. For the computation of the correlation the annual cycle was removed.*

	Helgoland	Elbe I	P11/P8	P15/P12
JAN	964	1186	877	866
FEB	918	1096	810	776
MAR	996	1205	875	842
APR	912	1157	830	705
MAY	926	1174	866	604
JUN	965	1116	832	526
JUL	1013	1166	866	570
AUG	1029	1174	854	557
SEP	976	1136	830	503
OCT	986	1156	857	674
NOV	919	1117	810	719
DEC	860	1169	836	824
SUM	11464	13852	10143	8166

Table 2.2: *Monthly distribution of measurements.*

Helgoland have been computed (Figure 2.2). Although there is a warm bias in the model, generally a good agreement can be inferred on interannual and longer time scales, that is, the bias is not changing in the course of time. For example, the relatively low temperatures at the end of sixties and seventies can be inferred from both, the model simulation and the observations. Also, the marked increase in SST in the last few decades is visible in the measurements as well as in the model data. Figure (2.3) shows a comparison of 20-year moving trends. Again, this comparison focuses on the longer time scales. It can be inferred, that simulated and observed 20-year trends show a high degree of similarity. In summary, the results indicate that the HAMSOM model in the applied

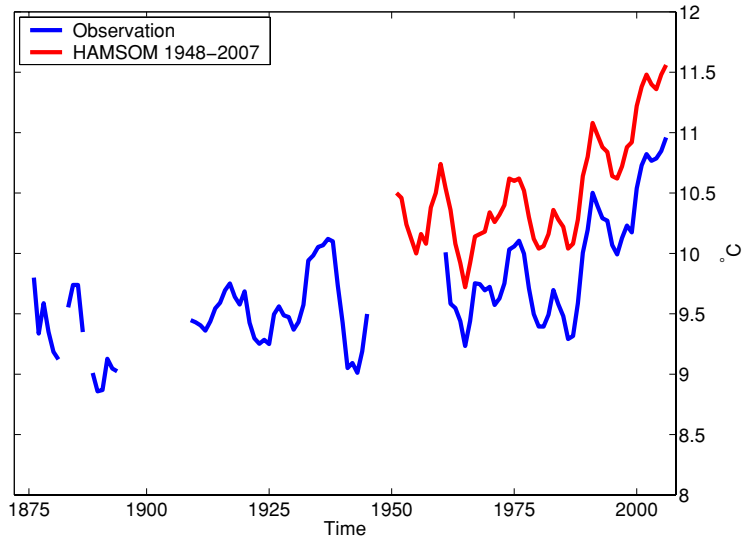

Figure 2.2: *5-year running means of observed (blue line) and simulated (red line) SST at Helgoland Roads.*

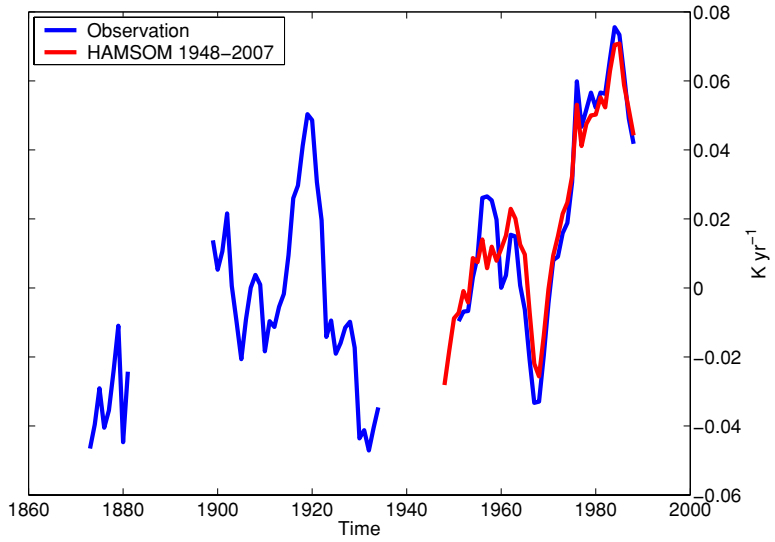

Figure 2.3: *Running 20-year-trends [K/yr] for Helgoland Roads derived from observations (blue line) and HAMSOM results (red line). Trend values have been associated with the first year of each 20-year window for which the analysis has been performed.*

configuration is able to reasonably simulate the observed temperature variations on long-time scales, at least at the near coastal locations considered here. However, Helgoland Roads is the only non-coastal station for which such a long time series is available.

3 Temperature analyses

Figure (3.1) shows the annual mean SST averaged over the entire North Sea together with the 3d temperature field averaged over the total model domain. Both, annual mean SST and 3d temperature average exhibit pronounced inter-annual and longer variations. The annual mean SST varies between $9.4\,^{\circ}C$ in 1979 and $11.1\,^{\circ}C$ in 2007, while the 3d temperature average ranges from $8.1\,^{\circ}C$ in 1979 to $9.0\,^{\circ}C$ in 2007. Both time series show a similar time behaviour, that is the fluctuations tend to be synchronous. Also, while both time series appear to be quasi-stationary until the early 1980s, a marked increase appears to occur afterwards.

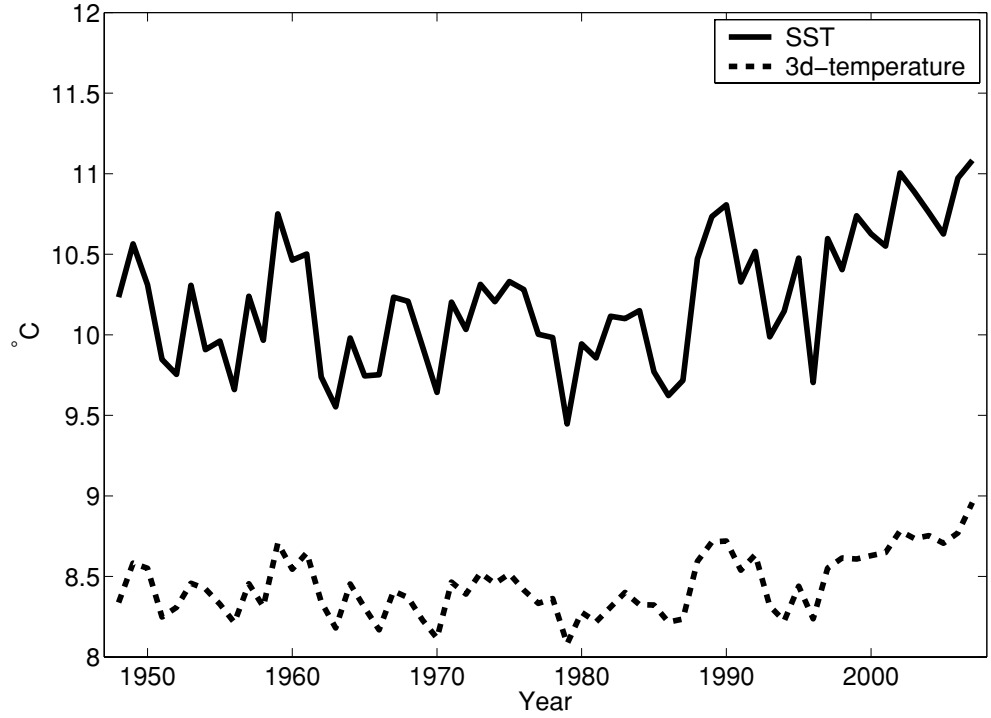

Figure 3.1: *Annual mean North Sea average sea surface temperature (solid line) and annual mean North Sea volume averaged temperature (dotted line).*

To elaborate whether this appears to be a large scale phenomenon linear SST trends for the two periods 1951-1982 and 1983-2007 have been computed for every model grid point (Figure 3.2). It can be inferred, that during the first period no visible trend occurred for the entire North Sea. This

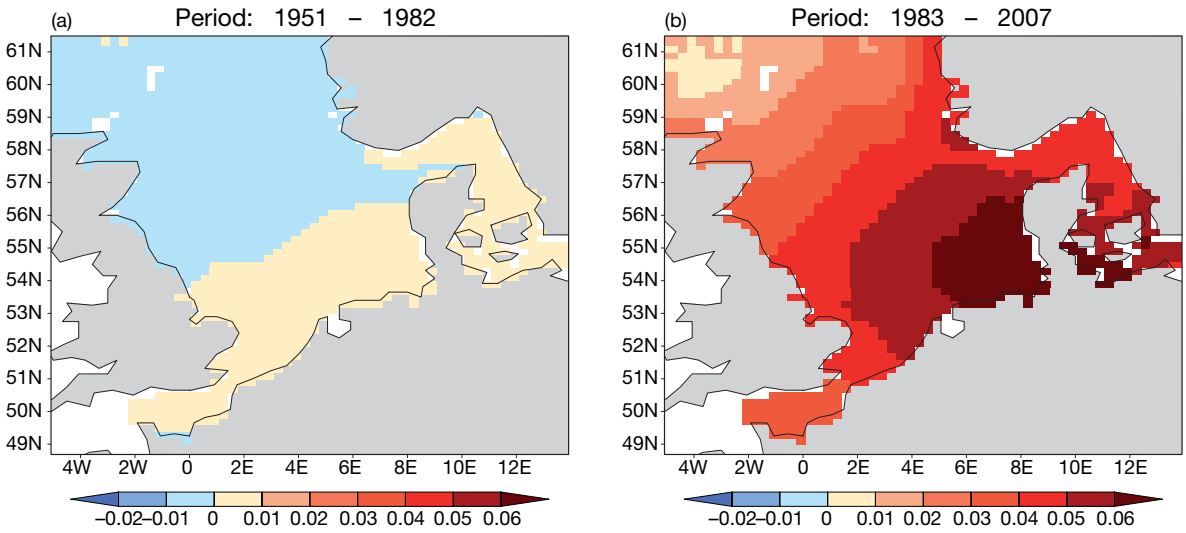

Figure 3.2: *Linear trends 1951-1982 (a) and 1983-2007 (b) of SST [K yr^{-1}].*

result changes considerably when considering the second period after 1983. Here, SST increases of up to $0.6\,K$ per decade are obtained that are most pronounced in the German Bight. In the central North Sea still trends of about $0.4 - 0.5\,K$ per decade are obtained, while they are considerably smaller ($0.1 - 0.3\,K$/decade) in the Northern North Sea near the Atlantic entrance.

In the southern North Sea the documented trend corresponds to an increase in sea surface temperatures of about 1.5 K within the last 25 years. To examine to what extent this increase is unusual, running 20-year trends from model and observations have been determined for Helgoland (Figure 2.3). The resulting trends show strong long-term variability ranging from low values of about $-0.0471\,K\,yr^{-1}$ in the 1930s and maximum values of up to $0.0756\,K\,yr^{-1}$ in the early 1980s. When the entire time series is considered, the trend emerging in the early 1980s was found to be the highest recorded, although the latest values appear to be somewhat smaller. The mean value and the standard deviation 1874-2007 of the running 20-year trends are $0.006\,K\,yr^{-1}$ and $0.0316\,K\,yr^{-1}$ respectively. This indicates, that the trend emerging in the early 1980s appears to be outside 2 times the standard deviation emphasising the unusual character of this period. Trends could also be detected for bottom temperatures of the North Sea (Figure 3.3). In the northern North Sea, bottom temperatures varied between $6\,^{\circ}C$ and $10\,^{\circ}C$, in the southern North Sea between about $3\,^{\circ}C$ and $18\,^{\circ}C$. In the southern North Sea, stronger warming can be inferred for both, during the cold and the warm seasons.

The spatial monthly mean SST for the period of 1961 to 1990 is shown in Figure A.1. Highest SST gradients are shown for the coastal areas. Offshore the variability of the seasonal cycle is lower. The climate pattern for the period of 1971 to 2000 (Figure A.2) is in principle similar to Figure (A.1), but in some specific points are changes.

In Appendix (Figure A.3 – A.7) the annual mean SST is shown. There is a high variability in the annual mean sea surface temperature. Notably, in the southern North Sea a high temperature gradient exists close to the coast evolving every year. Due to a constant climatological forcing at the open

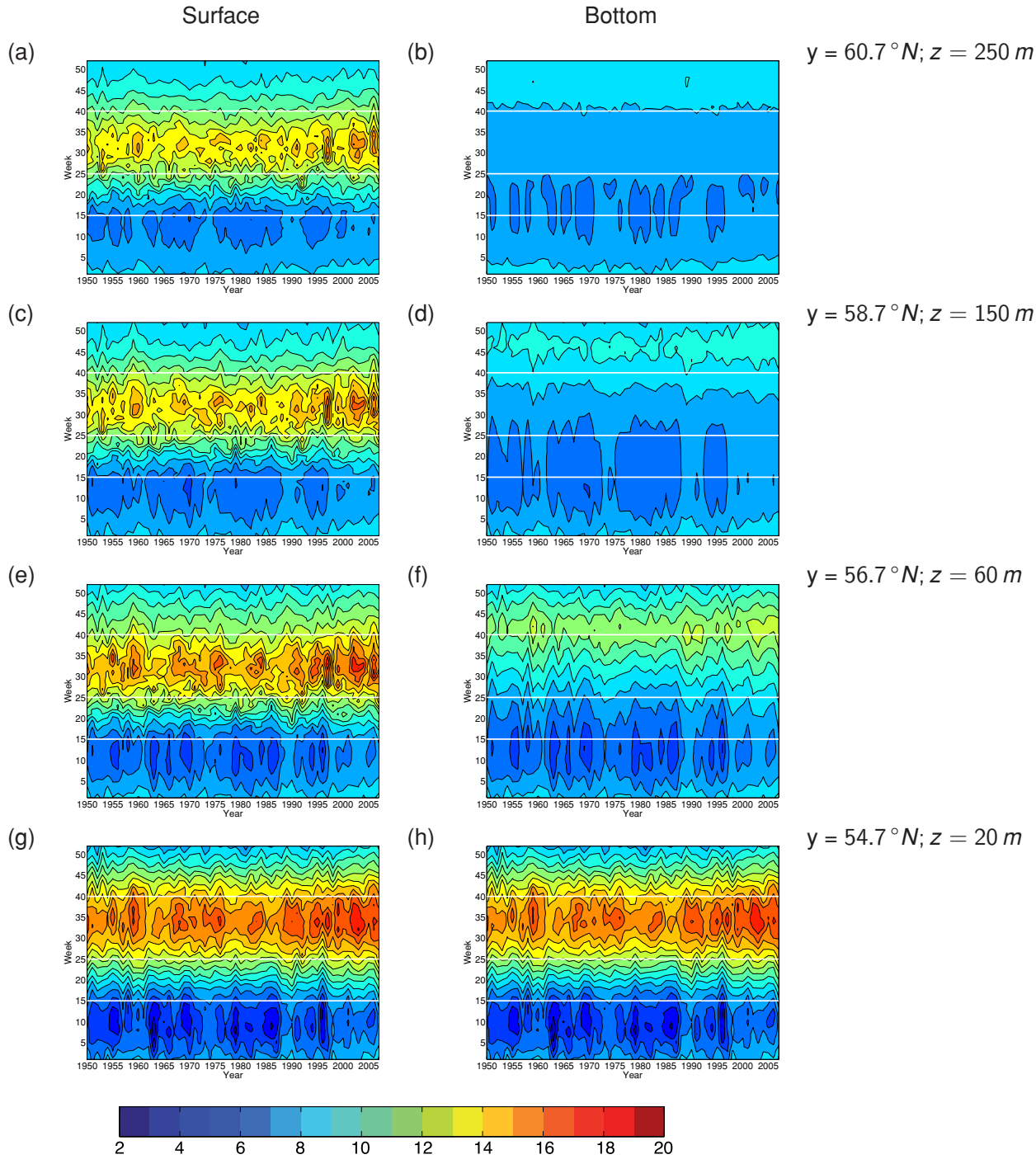

Figure 3.3: *Thermo-isopleth diagram of weekly temperature time series along a north-south cross section at* 3.25 °*E from north (*60.7 °*N, top) to south (*54.7 °*N, bottom) in* 2 ° *steps. Sea surface temperature (left; a,c,e,g); bottom temperature (right; b,d,f,h). White lines are artificial lines for orientation.*

boundaries, it can be concluded that in this study the main variability of the main heat forcing of the North Sea occurs via the atmosphere. Pohlmann (2003) found out, that changing lateral temperature conditions have only a small influence on the temperature in the central and southern North

Sea. Obviously this part of the North Sea is mostly well mixed and thus reacts fast on atmospheric changes.
The anomalies of the monthly SST shown in Appendix (Figure A.8) indicate the occurrence of warm (e.g. 1959 - 1960; 1971 - 1976; 1989 - 2007, expect 1996) and cold periods (1951 - 1958; 1977 - 1988). Over the past years warmer months are more frequent than in the years before. Especially the winter and spring SSTs are higher than the respective climatological mean SST.

Similar pattern of the SST anomaly are shown for the air temperature in Figure (B.1). The Hovmöller diagram showing the anomaly of air temperature clearly demonstrates a positive trend of the air temperature during the last 25 years. The spatial distributions of the trends for air temperature given in Figure (B.2) confirm this change in the trend. The patterns of the air temperature trends are similar to the trends of the SST dipicted in Figure (3.2).

4 Thermocline

After the winter season the North Sea is generally well mixed. In spring the sea absorbs more solar radiation due to the higher altitude of the sun and less clouds. In turn the sea surface is heating up and a thermocline is developing. Through wind stress, turbulence is introduced which causes a downward mixing of warm water and partially erodes the thermocline or increases its depth.
In the following the thermocline is defined by the existence of a local vertical temperature gradient

$$\frac{\Delta T\,[K]}{\Delta z\,[m]} \geq 0.1\,\left[\frac{K}{m}\right] \tag{4.1}$$

where T represents temperature and z depth. Figure (4.1) shows the long-term changes and variability of thermocline structure as obtained from our HAMSOM simulation when integrated over the entire North Sea. There is considerable inter-annual variability in both, mean and maximum thermocline depth with maximum thermocline depth between $21\,m$ and $35\,m$. Mean thermocline intensity appears to be rather stationary over the years with values between 0.15 and $0.18\,K\,m^{-1}$ while the maximum thermocline intensity shows considerably stronger variations. Correlations between thermocline depth and intensity are small. On the contrary to SST and volume averaged temperatures no noticeable increasing trends after 1980 are visible. Similar conclusions hold for the first day of noticeable thermocline development (Figure 4.1c) and the number of days with average vertical temperature gradients above the given threshold of $0.2\,K\,m^{-1}$ (Figure 4.1d)
Two noticeable events can be inferred from Figure (4.1). In 1979 and 1996 severely cold winters have been observed. Consequently, in 1979 the formation of the thermocline started late and had only a short life time. The mean SST of the summer season was low, too. In the following year 1980 the thermocline development started late in the year, but the lifetime was relatively long. The mean thermocline depth was smaller than in the year before. Furthermore the cold water was still remaining from the winter season of 1979. In 1996 there was a similar situation, i.e. a cold winter in 1996 and a short lifetime of the thermocline.

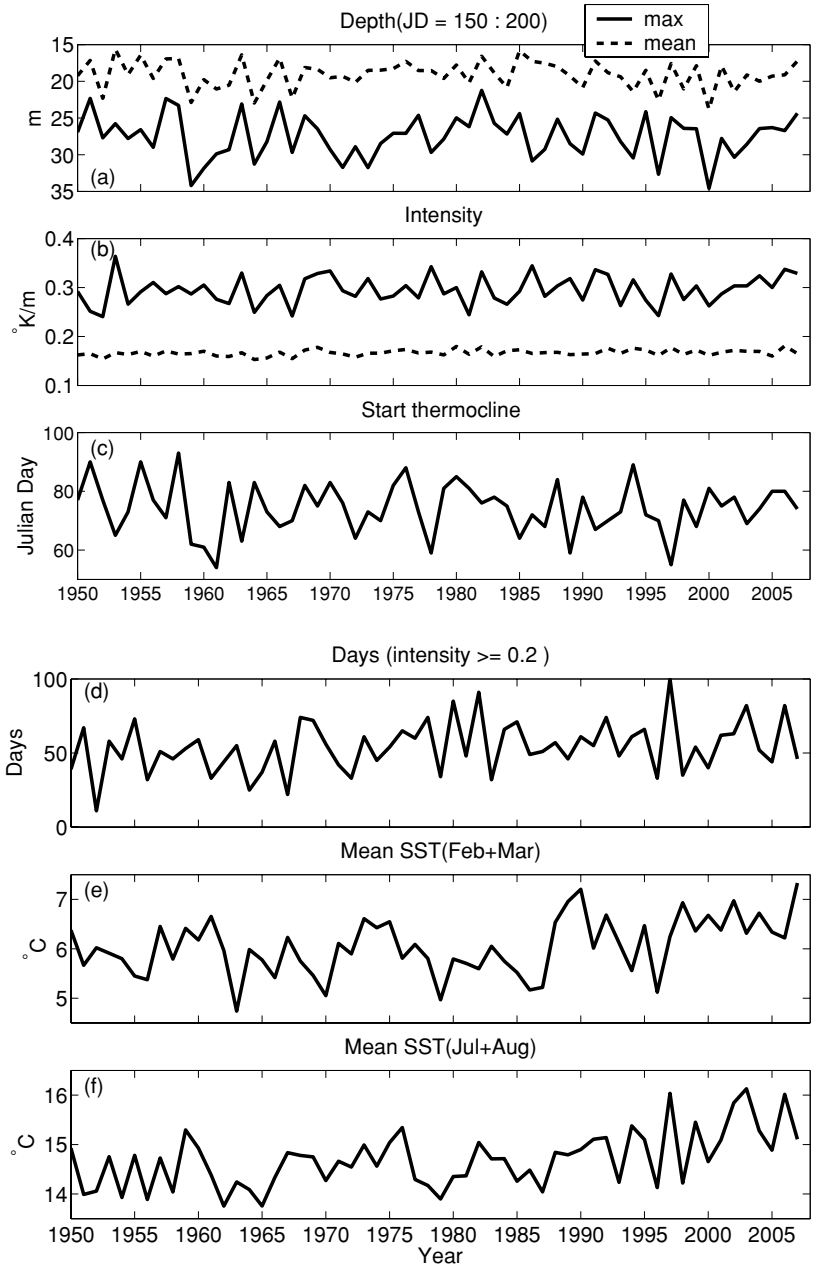

Figure 4.1: *Statistics of the volume averaged thermocline parameters 1950-2007. (a) Maximum (solid line) and average (dashed line) thermocline depth in m; (b) Mean (dashed) and maximum (solid line) thermocline intensity in K/m; (c) First Julian day with volume averaged thermocline stronger than* $\geq 0.1\ K\ m^{-1}$*; (d) Number of days with volume averaged thermocline intensity* $\geq 0.2\ K\ m^{-1}$*; (e) North Sea mean SST (February & March) in* $^\circ C$*; (f) North Sea mean SST (July & August) in* $^\circ C$*.*

5 Heat content

The heat content of the North Sea is mainly governed by solar and long-wave radiation as well as latent and sensible heat fluxes and by local vertical mixing. However the advective and horizontal diffusive heat fluxes may be relevant under certain conditions, too. The solar radiation depends on the declination of the sun and the cloud cover whereas the long-wave radiation depends on the difference between air and sea temperature and cloud cover. Sensible and latent heat fluxes are controlled by the difference of air and sea temperature, wind speed and water vapour pressure. The sum of all four fluxes yields the total heat flux into the ocean (Pohlmann, 2006). Positive heat fluxes occur predominantly during the spring and summer, while the heat fluxes are negative in autumn and winter.
The depth averaged heat content H of the North Sea is calculated by:

$$dH = \frac{1}{D} \int c_p \times \rho \times dT\, dz \tag{5.1}$$

where $c_p = 3980\, J\, kg^{-1}\, K^{-1}$ is the specific heat capacity for sea water (Feistel, 1993); ρ is the density of sea water and T is the potential temperature in layer z. The reference potential temperature is $0\,^{\circ}C$.

The annual and seasonal mean heat contents of the total North Sea are shown in Figure (5.1). In the annual mean, cold periods alternate with a minimum of $330 \times 10^5\, J\, m^{-3}$ with warm periods with a maximum of $366 \times 10^5\, J\, m^{-3}$.
Seasonally, heat content is largest in the summer months with inter-annual variability being largest in the winter ($46.6 \times 10^5\, J\, m^{-3}$) and spring season ($47.5 \times 10^5\, J\, m^{-3}$) while variability is only $31.6 \times 10^5\, J\, m^{-3}$ and $37.5 \times 10^5\, J\, m^{-3}$ in the summer and autumn, respectively. The temporal variability of the annual mean heat content is therefore mainly influenced by the winter and spring heat fluxes. The mean heat content from spring (April - June) is partly driven by the North Atlantic Oscillation index (NAO) from Hurrell (1995) indicated by a correlation of 0.48 between both time series. As for temperatures, there is no trend noticeable until the early 1980s while it becomes significantly positive afterwards (Table 5.1).

As for temperatures local linear trends for the two periods 1951-1982 and 1983-2007 have been computed for every model grid point (Figure 5.2). As for temperature, trends are small during the

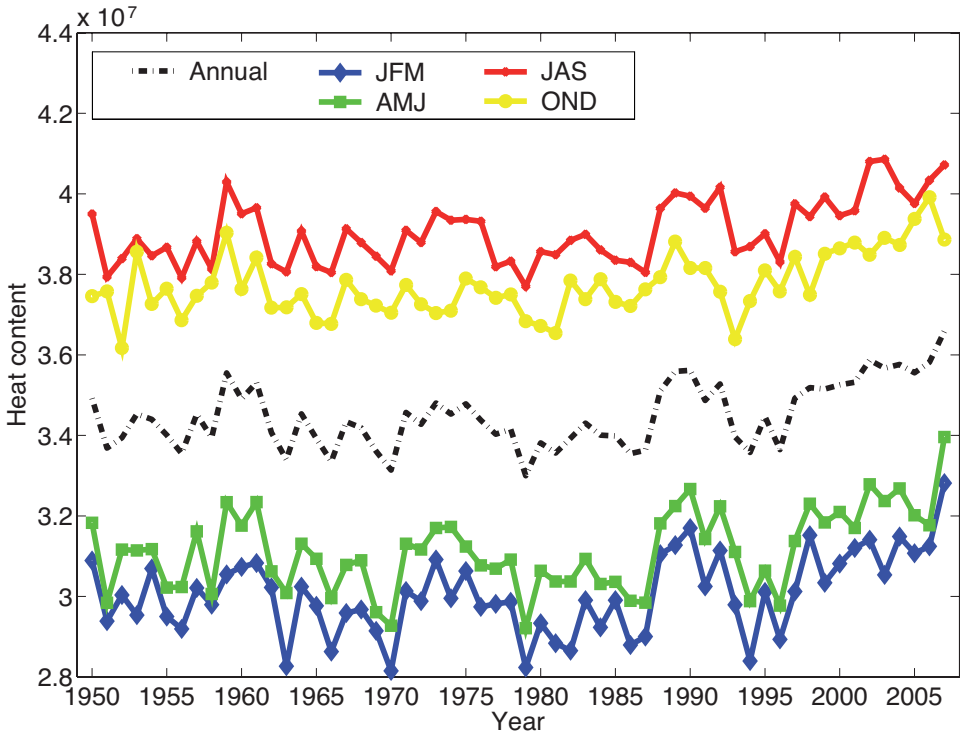

Figure 5.1: *Annual (black) and seasonal (JFM-blue, AMJ-green, JAS-red, OND-yellow) mean North Sea heat content in* $10^7\ J\,m^{-3}$.

	1951 - 1982	1983 - 2007	1951 - 2007
January - March	-0.22×10^5	0.81×10^5	0.23×10^5
April - June	-0.13×10^5	0.90×10^5	0.24×10^5
July - September	0.03×10^5	0.74×10^5	0.27×10^5
October - December	-0.13×10^5	0.74×10^5	0.23×10^5

Table 5.1: *Linear trends of North Sea heat content [J* $m^{-3}\ yr^{-1}$*] from 1951 – 1982; 1983 – 2007 and 1951 – 2007.*

first period and stronger during the second. Also, maximum values are again located in the German Bight (up to $3.0 \times 10^5\ J\,m^{-3}\,yr^{-1}$).

In a Hovmöller diagram (Figure 5.3) the monthly heat content during the period from 1950 to 2007 subtracted by the mean annual cycle from 1961 to 1990 is shown. On the x-axis the months from January to December are depicted and the y-axis represents the years from 1950 - 2007. There are periods with a negative anomaly (e.g. end of seventies and beginning of eighties) and periods with positive anomalies (from 1959 to 1961 and 1997 to 2007). The tendency to higher heat content in the approximately last 20 years is shown for nearly every month with a small interruption during the years 1995 to 1997. This concerns in particular the winter and spring season when the annual heat content has risen most significantly over the last 25 years (see also, Appendix C.6 and C.7).

The interannual variability of the mean annual heat content is shown from 1948 to 2007 in Appendix

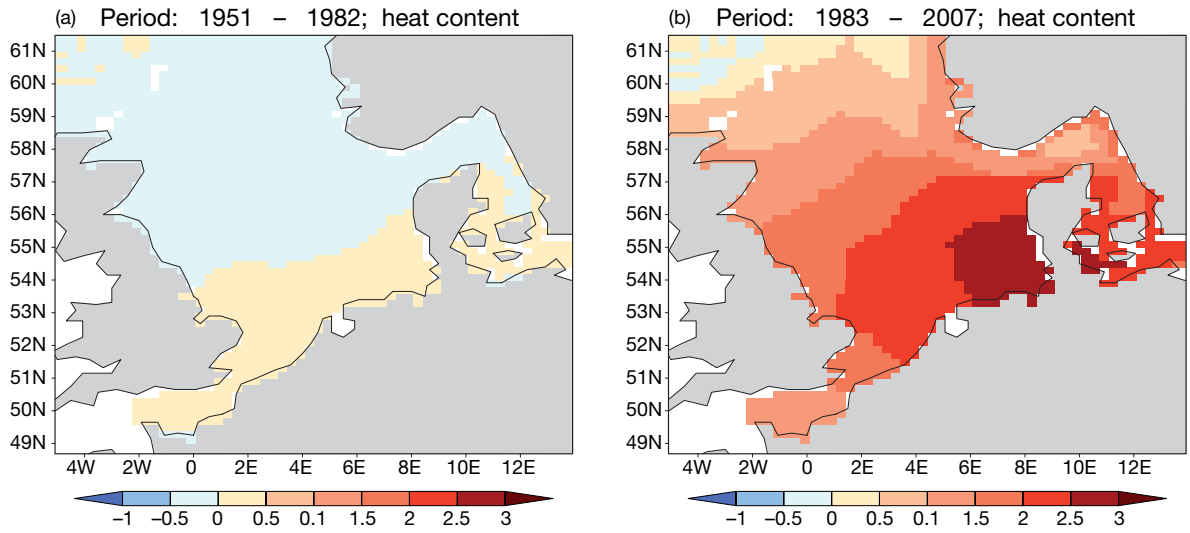

Figure 5.2: *Linear trends 1951-1982 (a) and 1983-2007 (b) of North Sea heat content [$10^5\ J\ m^{-3}\ yr^{-1}$].*

(Figure C.1 - C.5). In the shallow coastal areas the mean heat content is higher than in the deep areas. In Figures (C.1 - C.5) the mean annual heat content is calculated for each column. The influence of local atmospheric processes is higher in the shallow well mixed areas (southern North Sea) than in areas with deep bathymetry (northern Atlantic entrance). The heat content varies from year to year and becomes notably higher in the southern North Sea in the last years.

The heat content depicted in Figures (C.6 & C.7) represents the development of the winter heat content. The period of 1972 to 1983 represents a cold period and from 1996 to 2007 a warm period. In cold winters (e.g. 1976 - 1982 and 1996) the heat content is very low in the Geman Bight and Kattegat, whereas the deep areas like the Norwegian Trench are represented by a higher heat content as the surrounding areas. In summer it's vice versa. The well mixed shallow areas become warmer and the heat content is higher in the southern North Sea than close to the North Sea shelf break (Figure C.8 & C.9). Near the shelf break the heat content varies between $250 \times 10^5\ J\ m^{-3}$ and $550 \times 10^5\ J\ m^{-3}$ during the year. In the German Bight the heat content varies between $0 \times 10^5\ J\ m^{-3}$ and $900 \times 10^5\ J\ m^{-3}$. For all heat content calculations is the reference potential temperature $0\,^{\circ}$C.

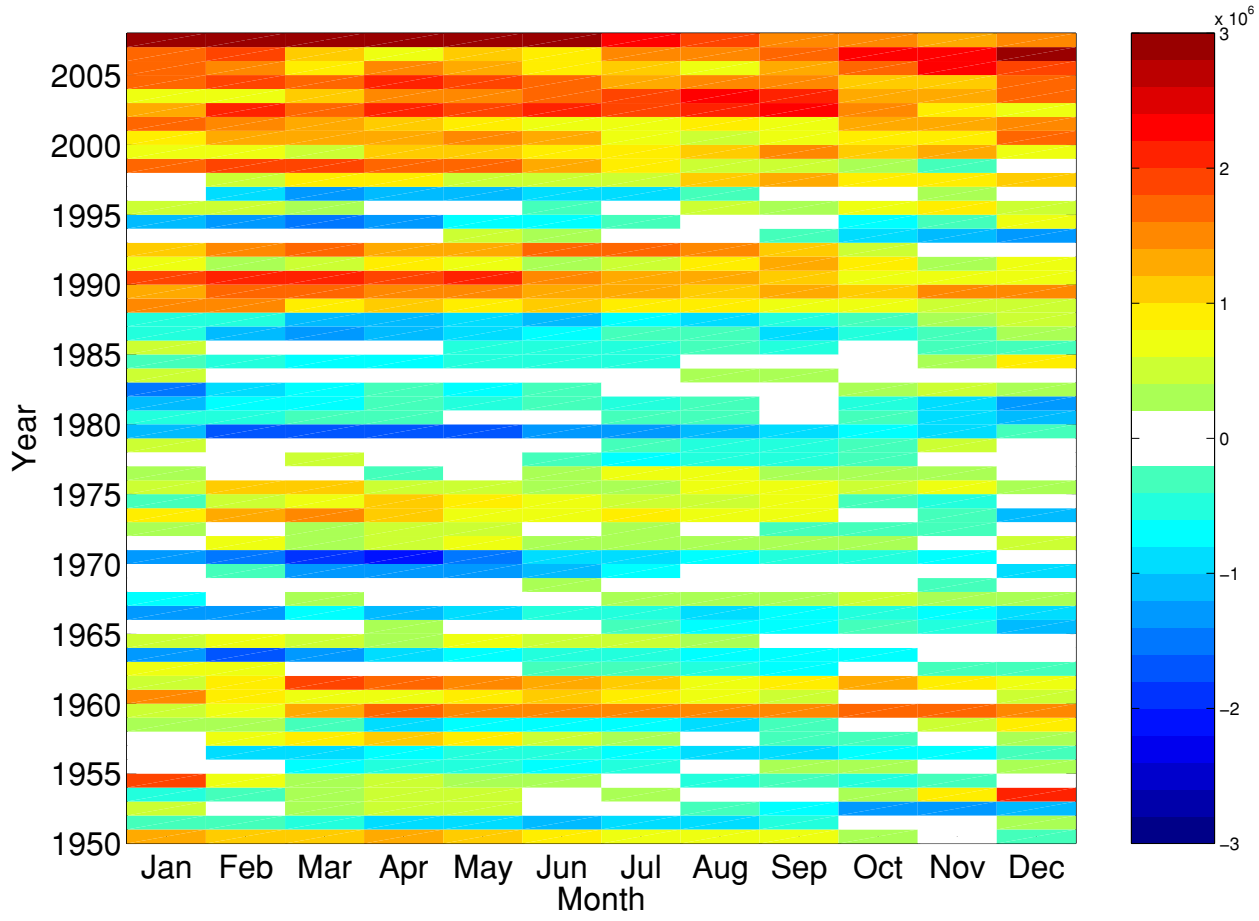

Figure 5.3: *Anomaly of monthly mean heat content [10^6 J m^{-3}].*

6 Sensitivity study

In the previous sections long-term changes in North Sea temperature, heat content and thermocline structure 1948-2007 were analysed. For heat content and temperatures a noticeable increase in 20-year trends during the mid 1980s has been identified that is most pronounced in the German Bight and visible also in observations at Helgoland.
As the model well reproduces the observed conditions, it provides a valuable tool to design sensitivity experiments to elaborate on the causes of these observed changes. Here the main idea is as following: The simulated long-term changes agree reasonably well with the observed ones. In the model, these changes must be caused by corresponding changes of either one or any combination of the forcing variables driving our long-term simulation, that is, air temperature, cloud cover, wind and humidity. Therefore experiments were designed, in which *one* forcing variable was set to its climatological mean values. The latter are calculated according to Equation (6.1) and hence include the full annual cycle. In order be able to attribute the occuring changes to a single cause all other forcing parameters were kept unchanged (Table 6.1).

	Forcing				
Name	Air temperature	Cloud	Wind	Sea level pressure	Humidity
Control run	NCEP	NCEP	NCEP	NCEP	NCEP
Air temperature	Climate mean	NCEP	NCEP	NCEP	NCEP
Cloud cover	NCEP	Climate mean	NCEP	NCEP	NCEP
Wind calm	NCEP	NCEP	NCEP 1958	NCEP 1958	NCEP
Wind moderate	NCEP	NCEP	NCEP 1957	NCEP 1957	NCEP
Wind storm	NCEP	NCEP	NCEP 1990	NCEP 1990	NCEP

Table 6.1: *List of sensitivity experiments*

In order to obtain a climatological forcing, the mean value at every time step (every 6h) over 60 years of the forcing data was calculated as:

$$\overline{f_c(t)} = \frac{\sum_{a=1948}^{2007} f(a,t)}{60} \qquad t = 1, 365\,(366)\ \times 4 \tag{6.1}$$

where *a* denotes the year, *t* the 4-daily NCEP output time steps and *f* the corresponding forcing variable. For wind, a slightly different strategy was adopted. Here, wind and sea level pressure from one year representing either strong, moderate or calm conditions over the North Sea is used repeatedly for the entire simulation period from 1948-2007. In particular, 1990 was used to represent a strong, 1957 a moderate and 1958 a calm wind condition year.
The results of the five experiments and the 'control run' are shown in Figure (6.1). The maximum of the annual mean thermocline depth integrated over the North Sea is displayed in the first diagram of Figure (6.1). Remarkably the depth of the thermocline is strongly dependent on the wind situation. The experiments with changing wind stress and sea level pressure strongly deviate from the others. The thermocline depths of the 'control run', climatological mean 'air temperature' and 'cloud cover' experiments are very similar. The position of the thermocline of the 'wind storm' experiment is the deepest. In 1990 strongest wind conditions occur in winter. In this experiment the cold water is strongly mixed down and a stable thermocline establishes at $22\,m$. The maximum depth is around $28\,m$. The experiments with 'wind moderate' and 'wind calm' show a shallower positions of the thermocline than all other experiments. The former experiments exhibit differences between the maximum of annual mean position of thermocline but the mean position itself is similar. The experiments with climatological mean 'air temperature' and 'cloud cover' reveal similar maximum mean depth position of the thermocline as the 'control run'. The results of the maximum temperature gradient are more heterogeneous and difficult to interpret (Figure 6.1b). The correlation of thermocline intensity (Table 6.2) of the experiments with the 'control run' varies between 0.66 and 0.70 for the wind experiments and between 0.85 and 0.88 for the other two experiments. The parameter 'area' is the area sum of model grid cells which exhibit a thermocline (Figure 6.1c). The experiments climatological mean 'air temperature' and 'cloud cover' have the highest correlations with the 'control run'. All experiments show no correlation for the beginning of the formation of the thermocline (Figure 6.1d). Reasonable correlations are found for the duration of a thermocline for the experiment climatological 'air temperature' and 'cloud cover'. All wind experiments show a smaller correlation. These results illustrate that the formation of thermocline depends mostly on the wind stress.

In Figure (6.2) the five year moving average of the annual mean heat content integrated over the North Sea of all experiments and of the 'control run' is shown. All runs except the experiment with climatological mean 'air temperature' show a strong periodicity of the heat content on the decadal scale and also the strong increase after the early 1980s. This leads to the conclusion, that the relevant forcing mechanisms for the observed decadal variability and change are missing, when the forcing parameter 'air temperature' is set to climatological values. In other words, it can be concluded that air temperature has a dominant influence on the heat content of the North Sea. Interestingly, the experiment with climatological mean 'cloud cover' forcing produces a higher heat content than the control run. In winter the climatological mean 'cloud cover' is larger than the respective cloud cover in cold winters. So the long-wave radiation is smaller than in cold winters with lower cloud cover. The experiment with high wind speed is an extremely artificial experiment. Normally, in cold winters a distinctive high pressure system prevails over Eastern Europe. So there exists a calmer wind situation over the North Sea domain. In the experiment 'wind storm' more cold water is mixed

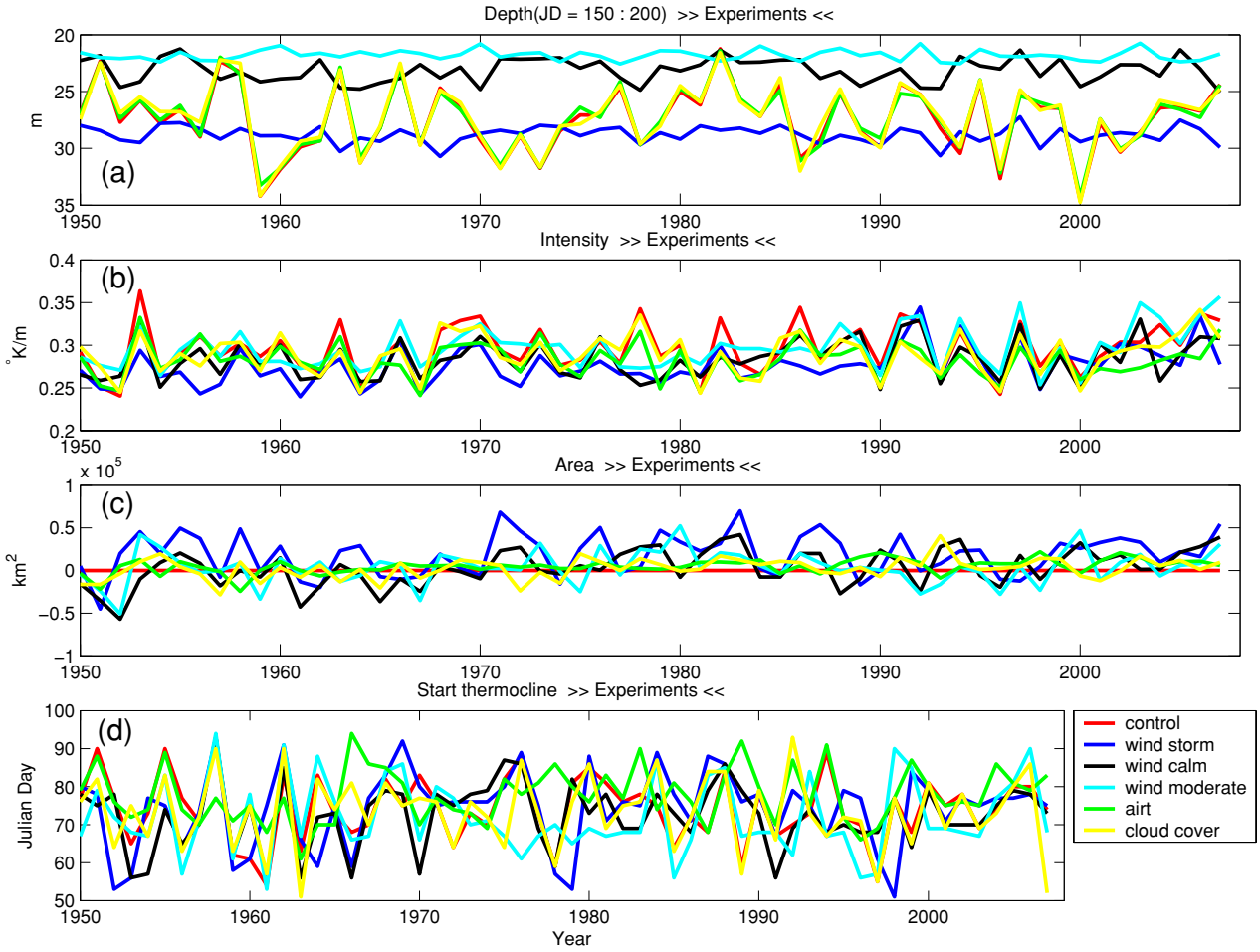

Figure 6.1: *Statistics of thermocline parameters: (a) Maximum Depth; (b) Intensity (c) Area (d) Thermocline onset; Results for the experiments 'control' red; 'wind storm' blue; 'wind calm' black; 'wind moderate' light blue; 'air temperature' green and 'cloud cover' yellow.*

down to deeper layers than in respective cold winters. In reality the winter of 1990 was relatively warm compared to the other winter and characterised by a westerly wind situation.

The trends of the heat content of all sensitivity studies are similar to the control run, expect for the experiment with the climatological mean 'air temperature'. Hence it can be inferred that the parameter air temperature explains about 75 % of the positive trend of the heat content in the last years, so it is the dominant physical forcing parameter for heat. Wind forcing and cloud cover only have a secondary influence on the observed long-term changes in North Sea heat content and temperature.

	AIR TEMPERATURE	CLOUD COVER	WIND CALM	WIND MODERATE	WIND STORM
max. depth	0.99	0.99	0.11	-0.11	0.06
mean depth	1.00	0.99	0.43	0.35	0.31
max. intensity	0.88	0.85	0.70	0.68	0.66
mean intensity	0.85	0.93	0.78	0.83	0.78
max. area	0.94	0.88	0.55	0.65	0.51
mean area	0.82	0.93	0.78	0.72	0.69
start thermocline	0.3	0.63	0.53	0.41	0.35
Days (intensity $\geq 0.2K\ m^{-1}$)	0.91	0.93	0.76	0.75	0.77

Table 6.2: *Correlations of the sensitivity study.*

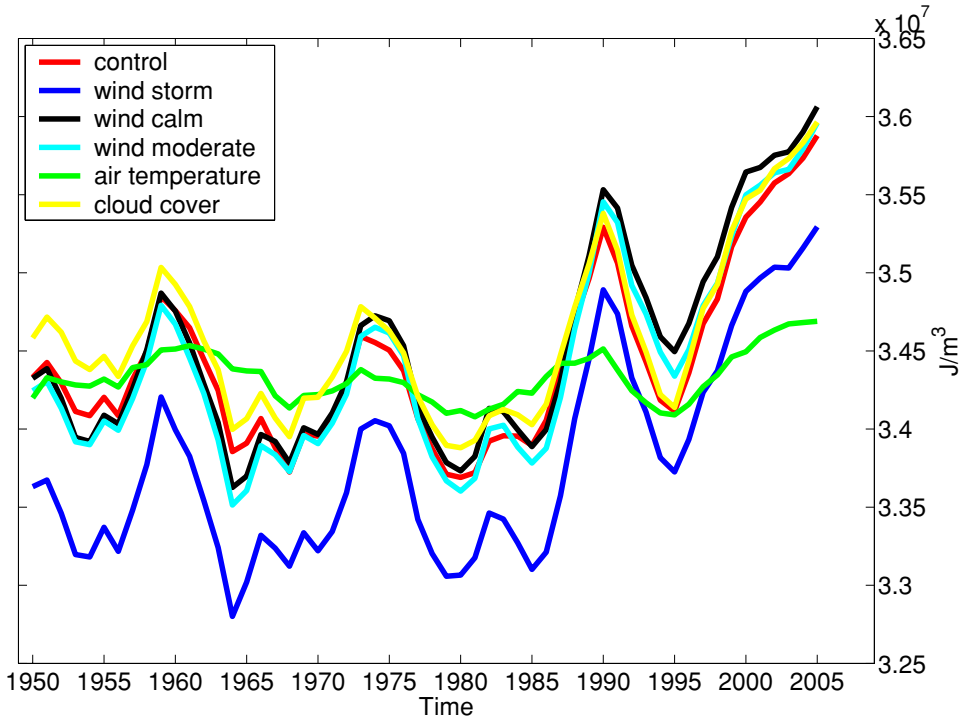

Figure 6.2: *Results from 5-years moving average of heat content from sensitivity experiments; 'control' red; 'wind storm' blue; 'wind calm' black; 'wind moderate' light blue; 'air temperature' green and 'cloud cover' yellow.*

7 Conclusion

Thermodynamic conditions in the North Sea for the period from 1948 to 2007 have been reconstructed at high spatial and temporal detail using the baroclinic shelf sea model HAMSOM. Comparison of model results with observations indicate that the model reasonably well reproduces observed conditions and variability on annual and longer time scales in the North Sea. Analysing the model data, pronounced interannual variability was found for North Sea temperatures, heat content and thermocline structure. While there have been only small changes before the early 1980s, model results indicate a considerable warming afterwards that is in agreement with long-term observations from Helgoland. The warming is most pronounced in the German Bight. Sensitivity experiments indicate that local air-sea interaction is the dominant driver responsible for the observed long-term changes.

The results are broadly consistent with earlier studies. In particular Becker and Pauly (1996) provided a correlation analysis between observed North Sea SST anomalies and the NAO index. They concluded that the observed SST variability in the German Bight is primarily a result of local atmosphere-ocean heat exchange which in turn depends on the stage of the large scale atmospheric circulation while oceanic advection plays a role only at the northern and southern open boundaries. With two years more of data and a slightly different methodology Dippner (1997) yields similar conclusions. Kauker (1999) studied the relation between North Sea inflow and North Sea SST anomalies based on a model reconstruction from 1979 to 1993. He also concluded that the observed SST anomalies are more a result of local atmosphere ocean interaction than of oceanic advection. Similarly, by varying lateral boundary conditions in an ocean model experiment Pohlmann (2003) showed that changing lateral temperature conditions have only a limited influence on the temperature in the southern North Sea and German Bight. Janssen (2002) performed a canonical correlation analysis between large scale sea level pressure and North Sea SST anomalies. He found that NAO like sea level pressure anomalies are positively correlated with warm North Sea SST anomalies and concluded that changes in the atmospheric large scale circulation modify air temperatures above the North Sea and as a result local sensible and latent heat fluxes.

In the present study, we have shown that North Sea temperature and heat content have changed considerably during the last few decades. In particular, strong increases were obtained after the early 1980s that are consistent with available observational records. Noteworthy, this period shows highest values of the entire duration of the Helgoland Road data set which was employed in our study. The data set obtained from our simulation comprises the 60 years from 1948 to 2007 and is

available every hour within this period. Hence we can expect that our simulation provides a reasonable tool to further study long-term changes in North Sea thermodynamics and that it may be of use and relevance for following up studies in particular in the field of marine biology or ecology.

Acknowledgements
The authors want to thank the DOD (German Oceanographic Data Centre) for providing Helgoland Roads data and for providing data from light vessels in the German Bight.
The Helgoland Roads Data are also provided by Biologische Anstalt Helgoland/Alfred-Wegener-Institut für Polar- und Meeresforschung.
NCEP Reanalysis data provided by the NOAA/OAR/ESRL PSD, Boulder, Colorado, USA, from their Web site at http://www.cdc.noaa.gov/.
Thanks to Peter Damm for preparing NCEP data and Mrs. Beate Gardeike for preparing some of the figures.

A. Water temperature

Mean monthly SST [$^{\circ}C$] from 1961 - 1990. Figure (A.1)
Mean monthly SST [$^{\circ}C$] from 1971 - 2000. Figure (A.2)
Mean annual SST [$^{\circ}C$] from 1948 - 1959. Figure (A.3)
Mean annual SST [$^{\circ}C$] from 1960 - 1971. Figure (A.4)
Mean annual SST [$^{\circ}C$] from 1972 - 1983. Figure (A.5)
Mean annual SST [$^{\circ}C$] from 1984 - 1995. Figure (A.6)
Mean annual SST [$^{\circ}C$] from 1996 - 2007. Figure (A.7)
Anomaly of monthly mean sea surface temperature [K]. Figure(A.8)

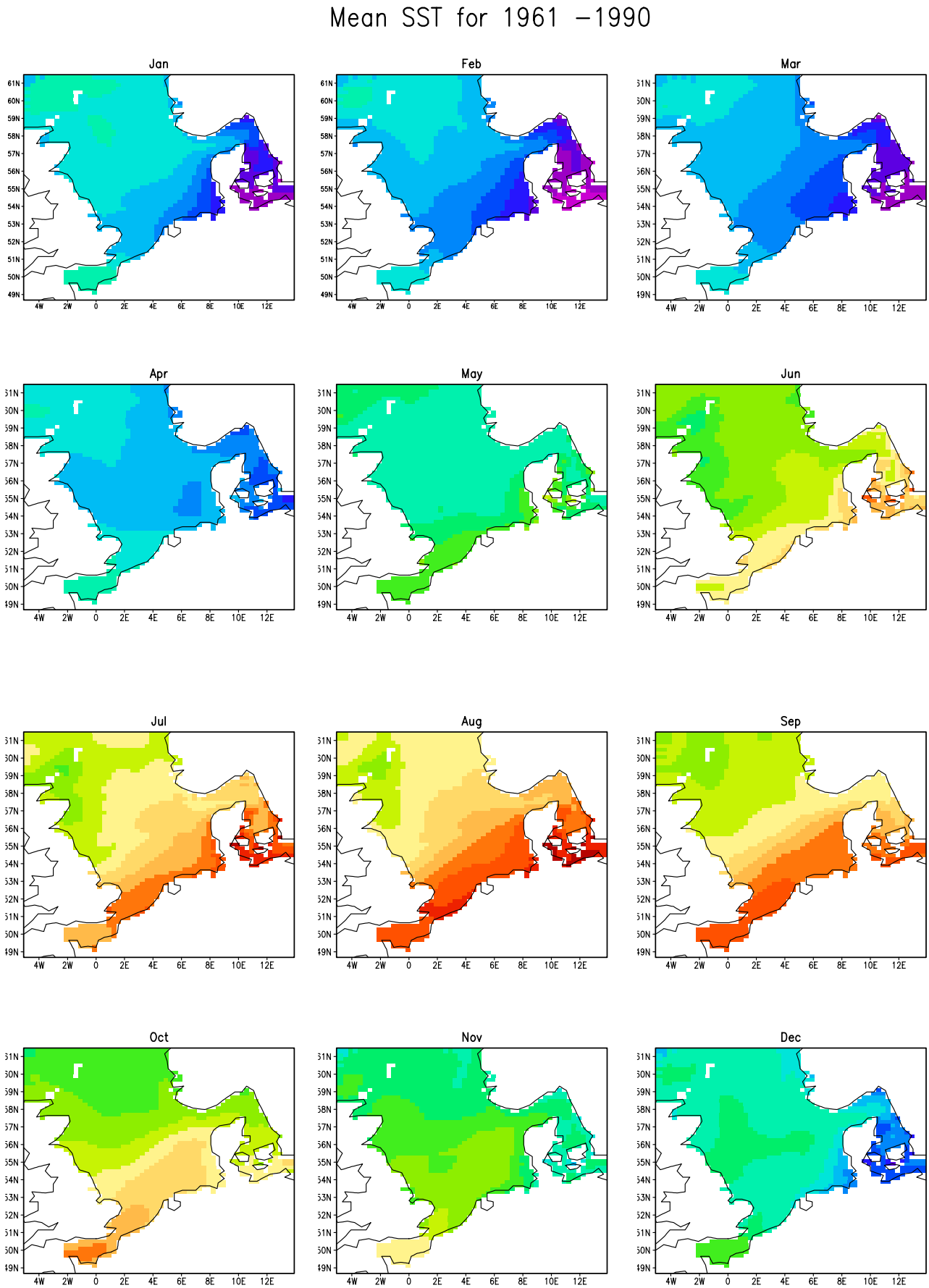

Figure A.1: *Mean monthly SST [°C] from 1961 - 1990.*

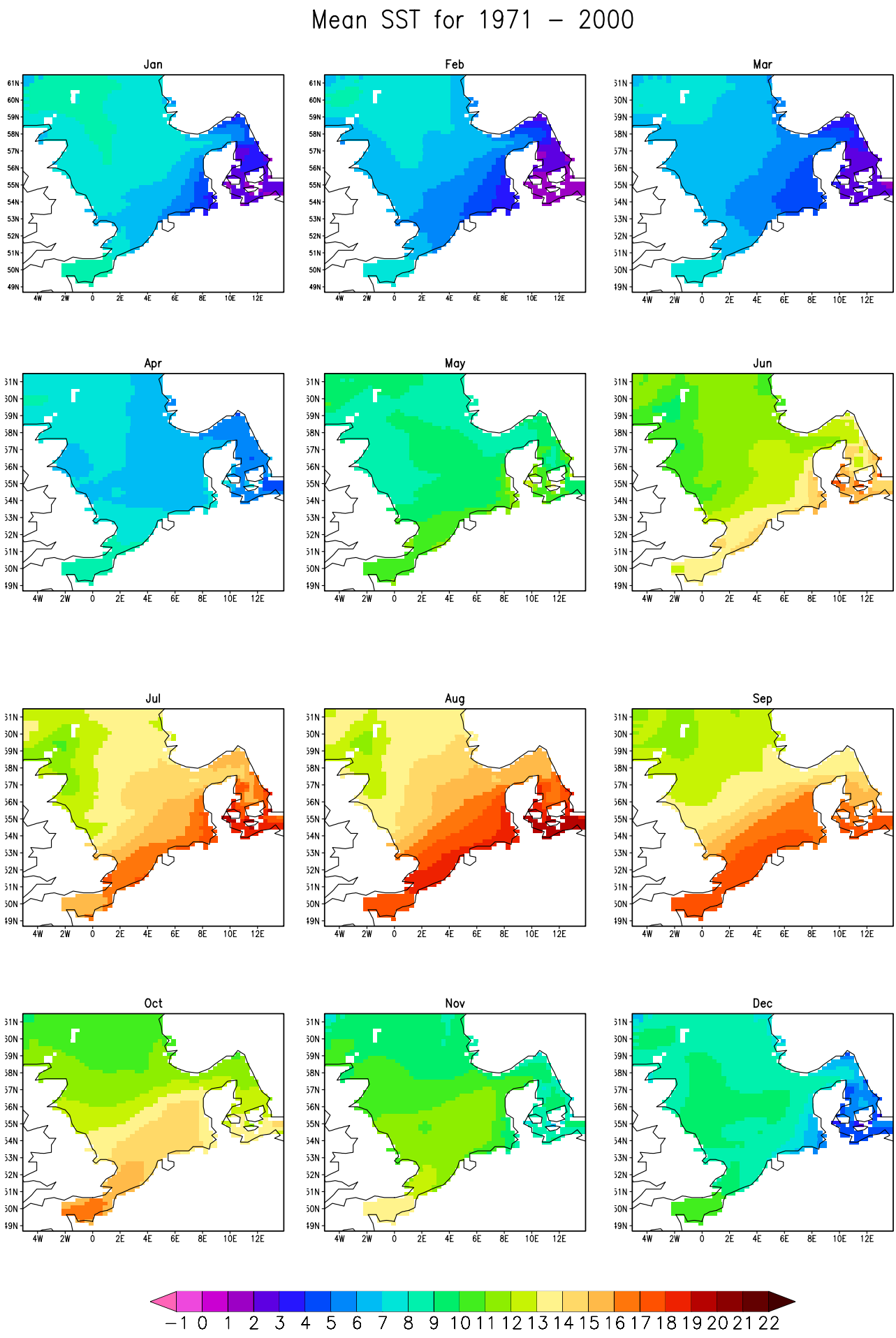

Figure A.2: *Mean monthly SST [°C] from 1971 - 2000.*

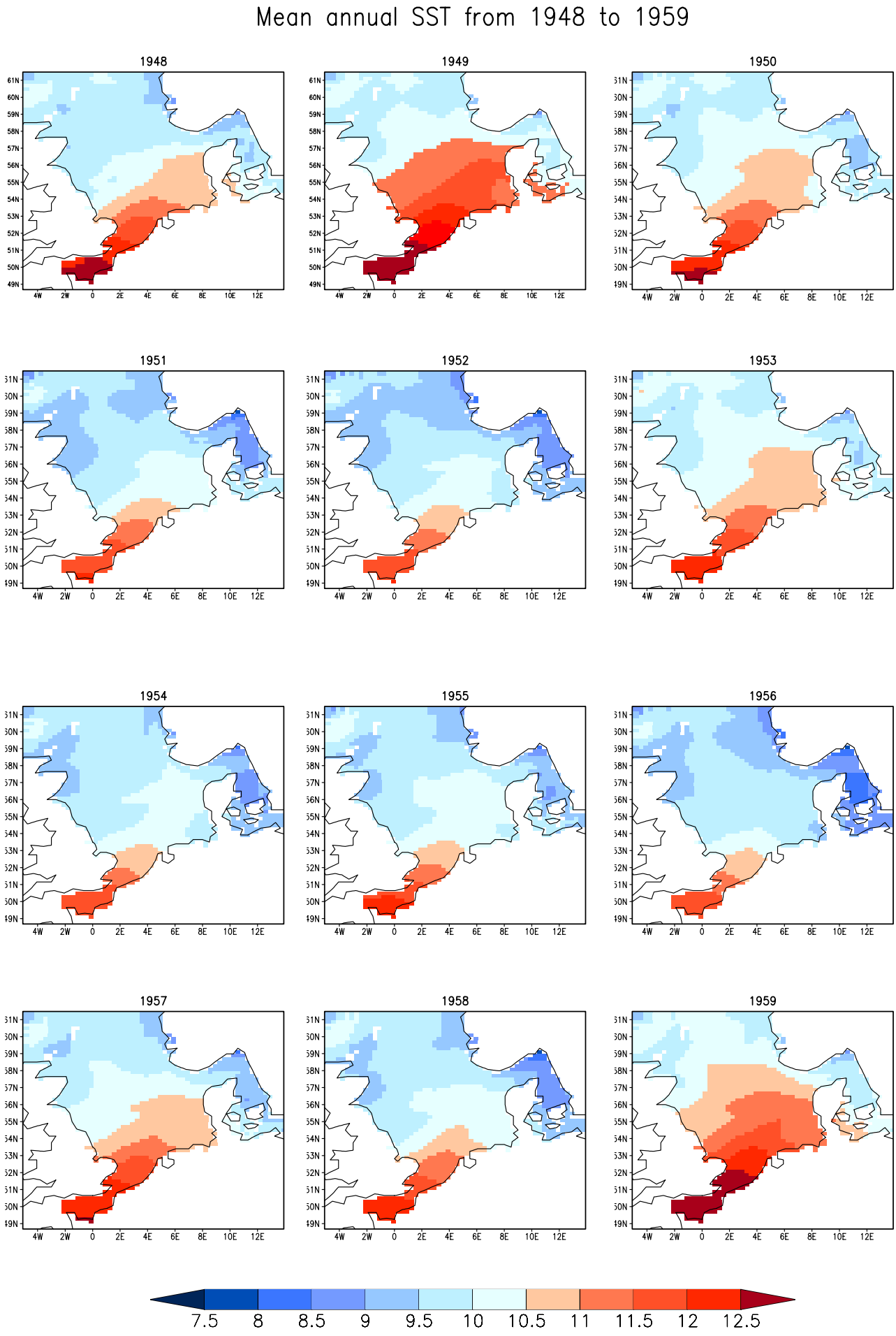

Figure A.3: *Mean annual SST [°C] from 1948 - 1959.*

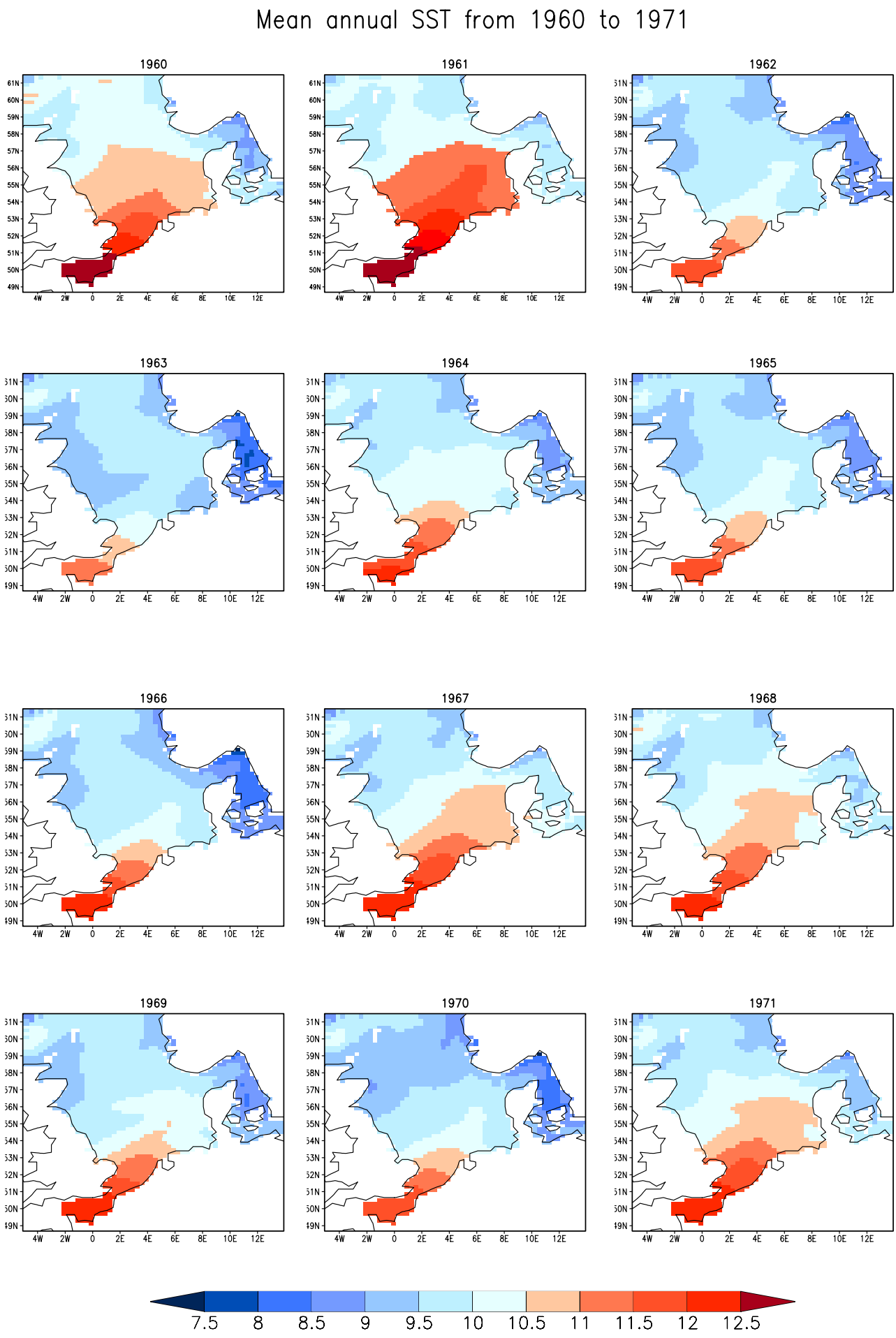

Figure A.4: *Mean annual SST [°C] from 1960 - 1971.*

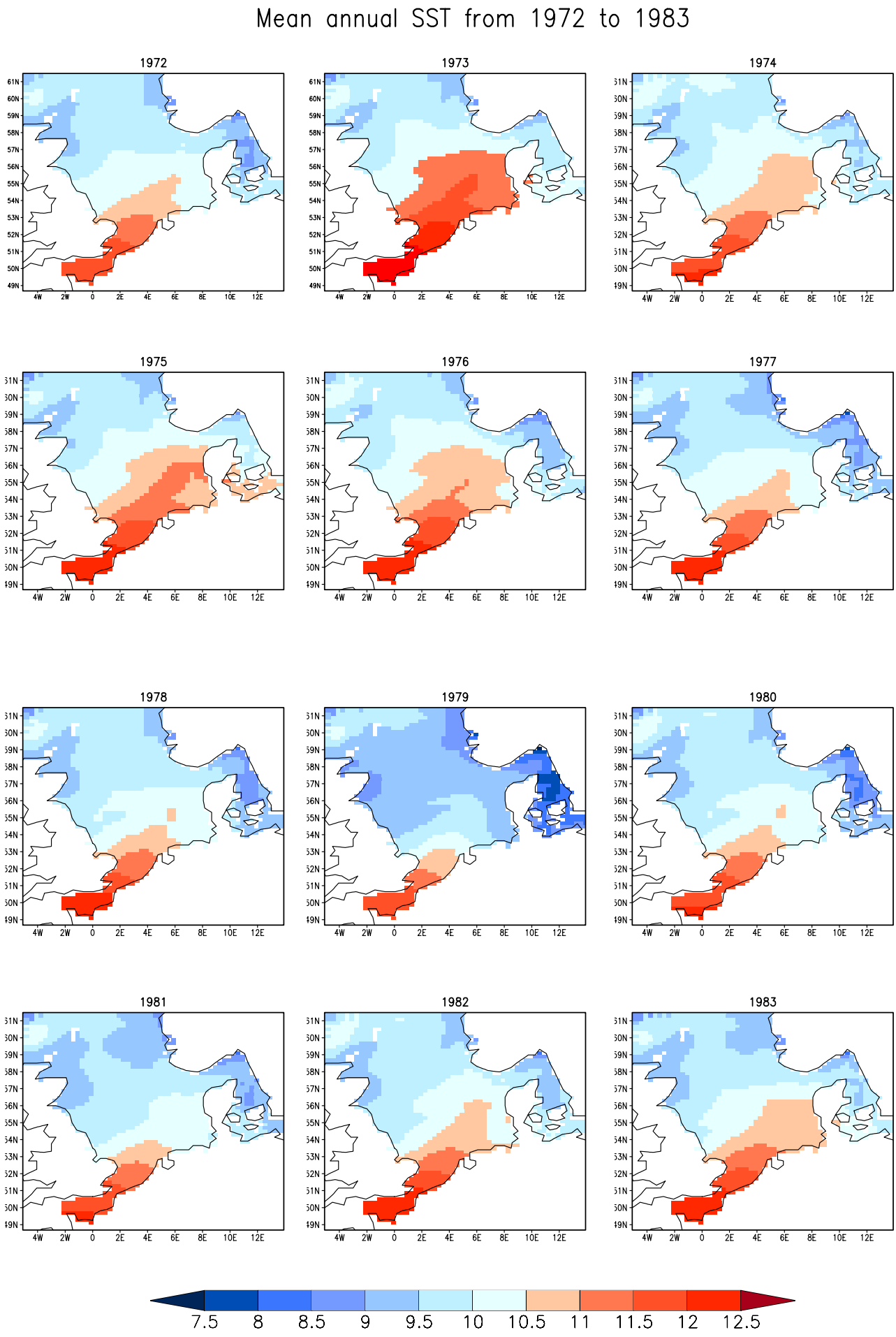

Figure A.5: *Mean annual SST [°C] from 1972 - 1983.*

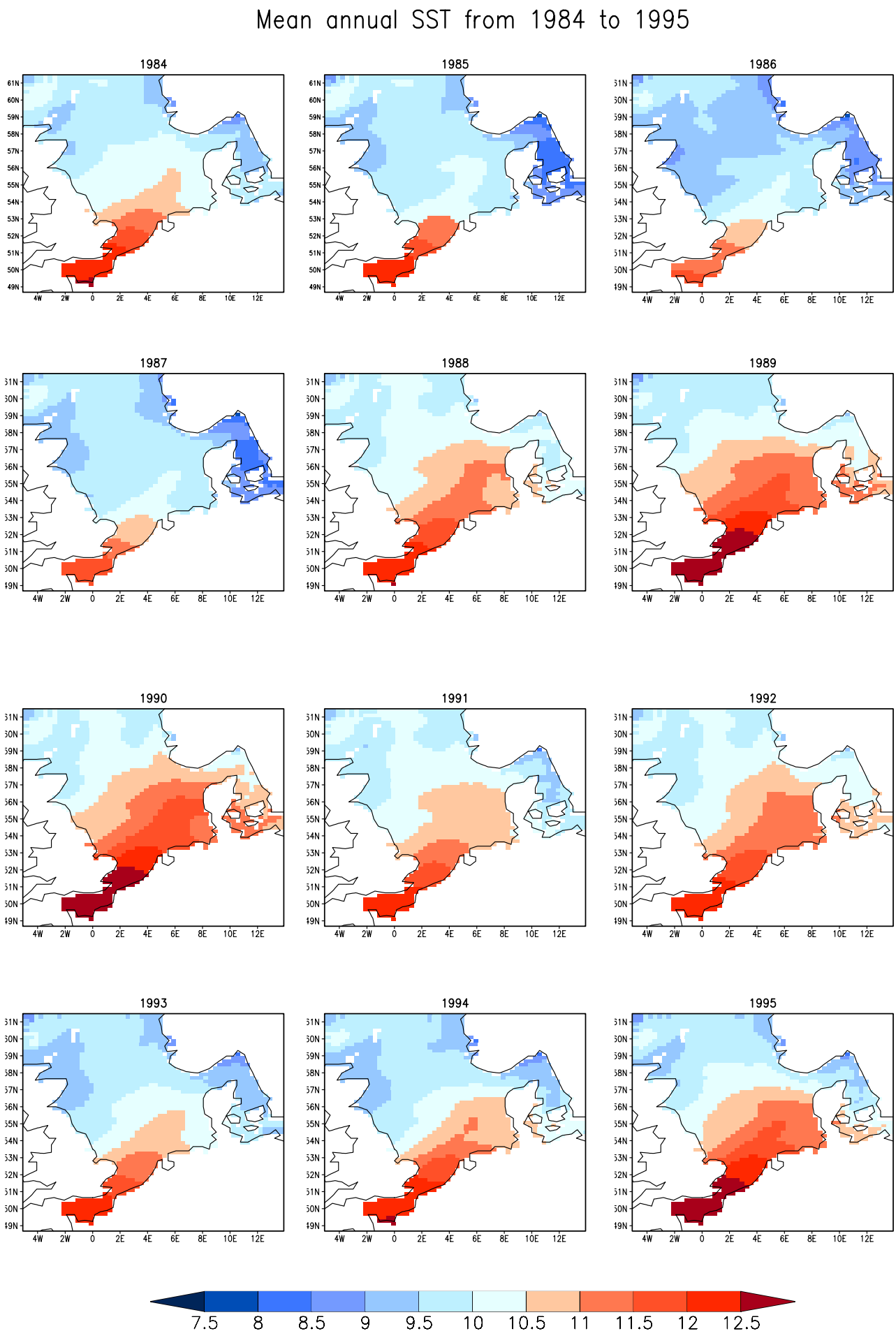

Figure A.6: *Mean annual SST [°C] from 1984 - 1995.*

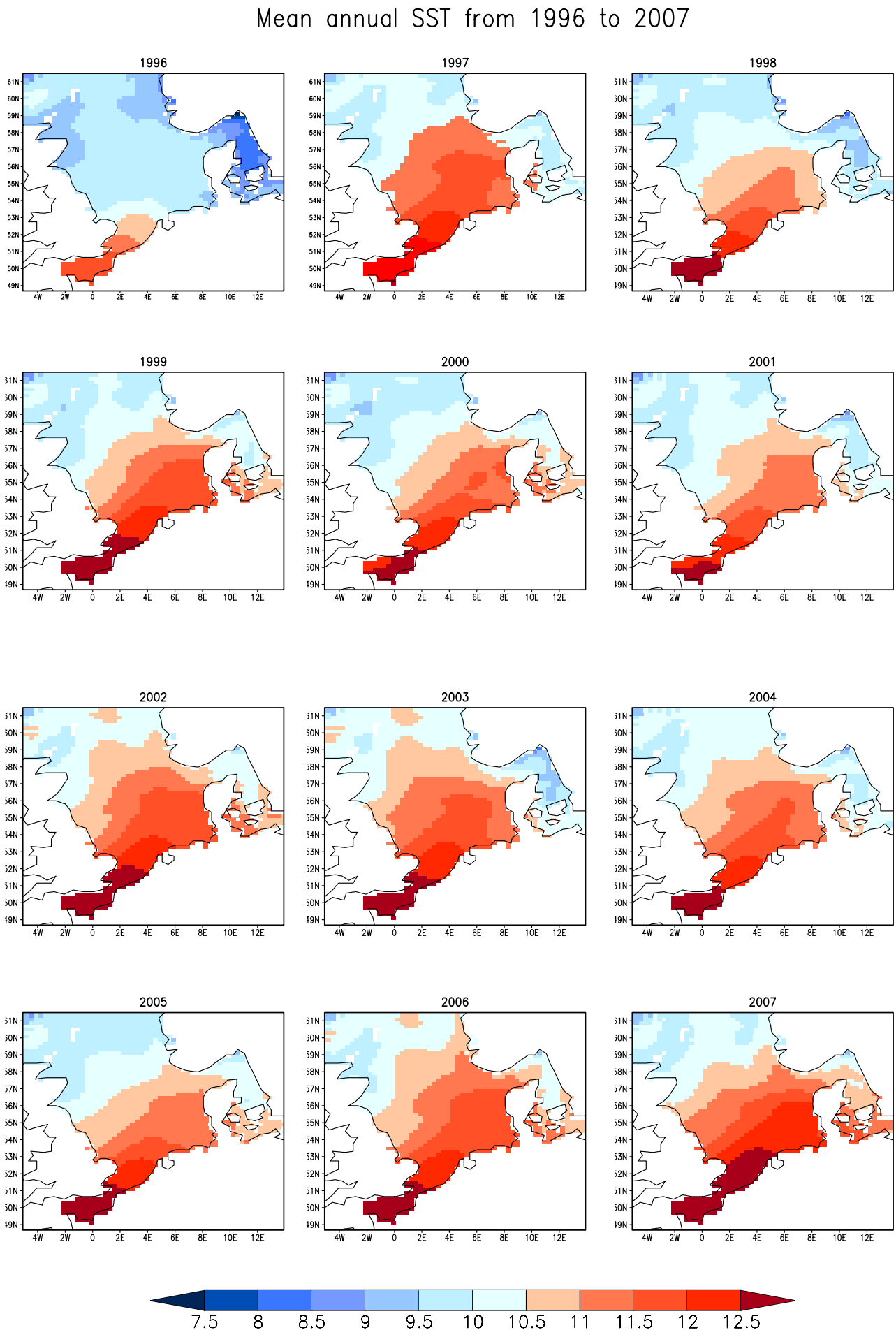

Figure A.7: *Mean annual SST [°C] from 1996 - 2007.*

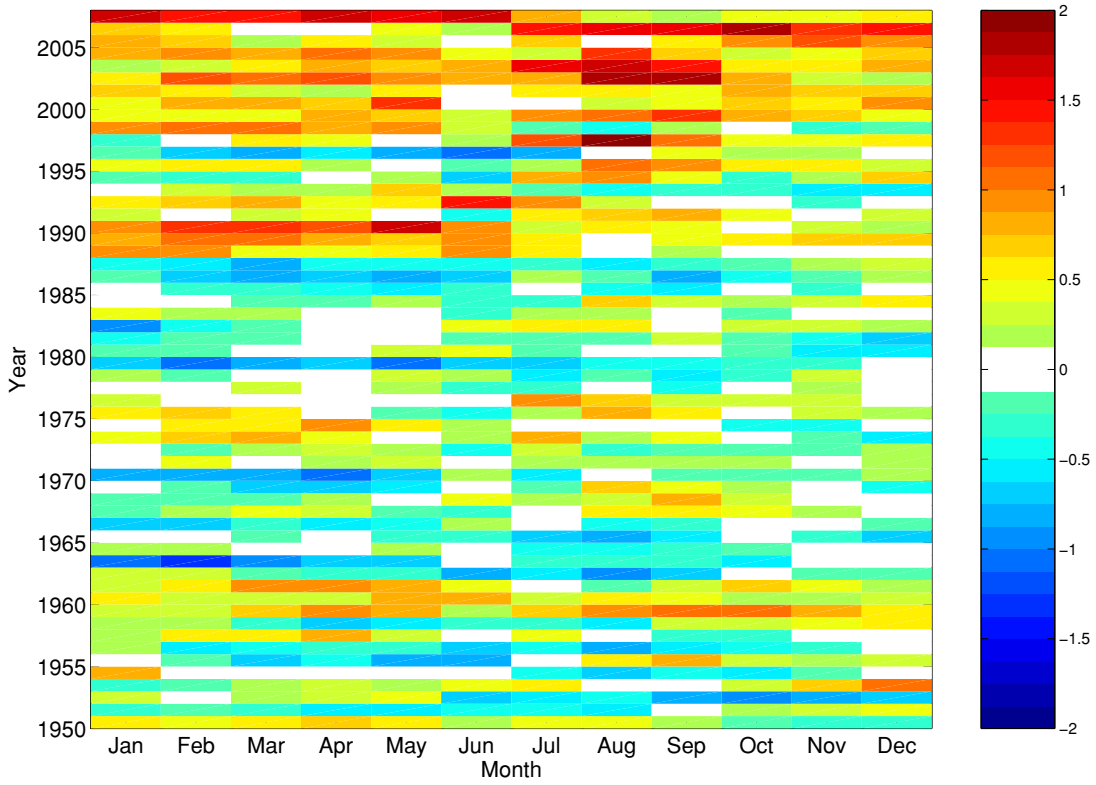

Figure A.8: *Anomaly of monthly mean sea surface temperature [K].*

B. Air temperature

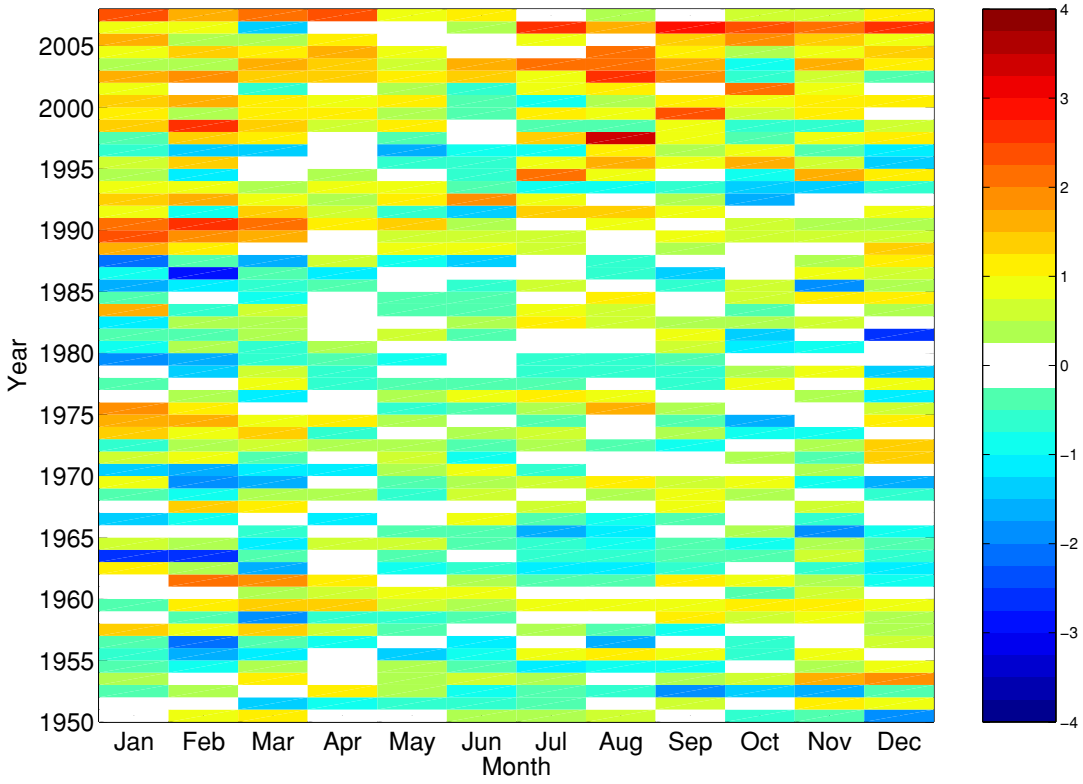

Figure B.1: *Monthly mean air temperature minus annual cycle [K].*

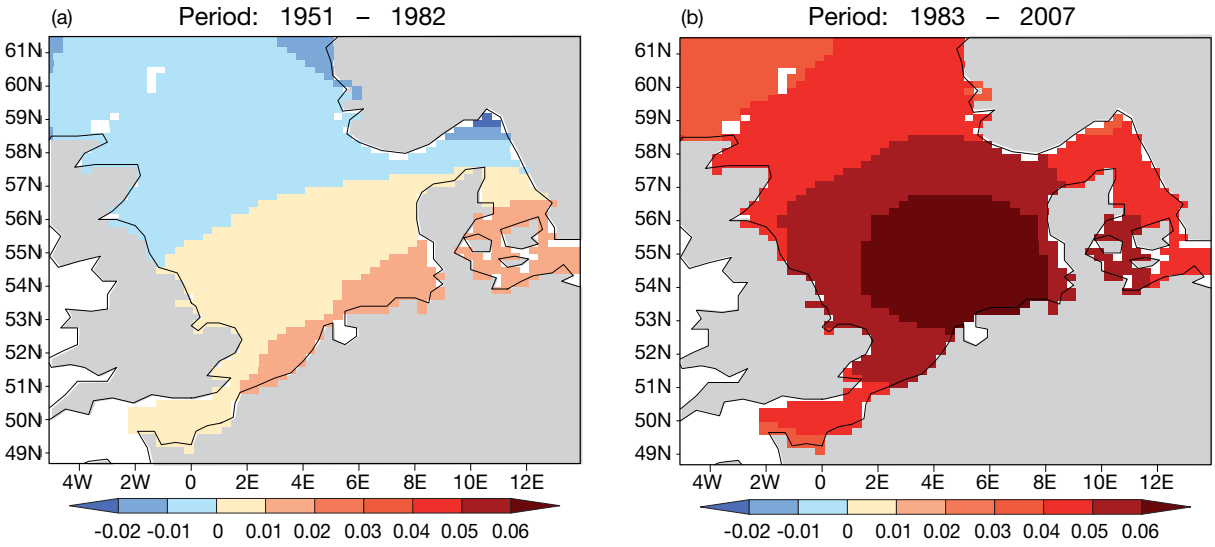

Figure B.2: *Trends of air temperature [K yr^{-1}] from 1951 to 1982 (a) and from 1983 to 2007 (b).*

C. Heat content

Mean annual heat content [10^5 $J\,m^{-3}$] from 1948 - 1959. Figure (C.1)
Mean annual heat content [10^5 $J\,m^{-3}$] from 1960 - 1971. Figure (C.2)
Mean annual heat content [10^5 $J\,m^{-3}$] from 1972 - 1983. Figure (C.3)
Mean annual heat content [10^5 $J\,m^{-3}$] from 1984 - 1995. Figure (C.4)
Mean annual heat content [10^5 $J\,m^{-3}$] from 1996 - 2007. Figure (C.5)
Mean heat content [10^5 $J\,m^{-3}$] for February from 1972 - 1983. Figure (C.6)
Mean heat content [10^5 $J\,m^{-3}$] for February from 1996 - 2007. Figure (C.7)
Mean heat content [10^5 $J\,m^{-3}$] for August from 1972 - 1983. Figure (C.8)
Mean heat content [10^5 $J\,m^{-3}$] for August from 1996 - 2007. Figure (C.9)

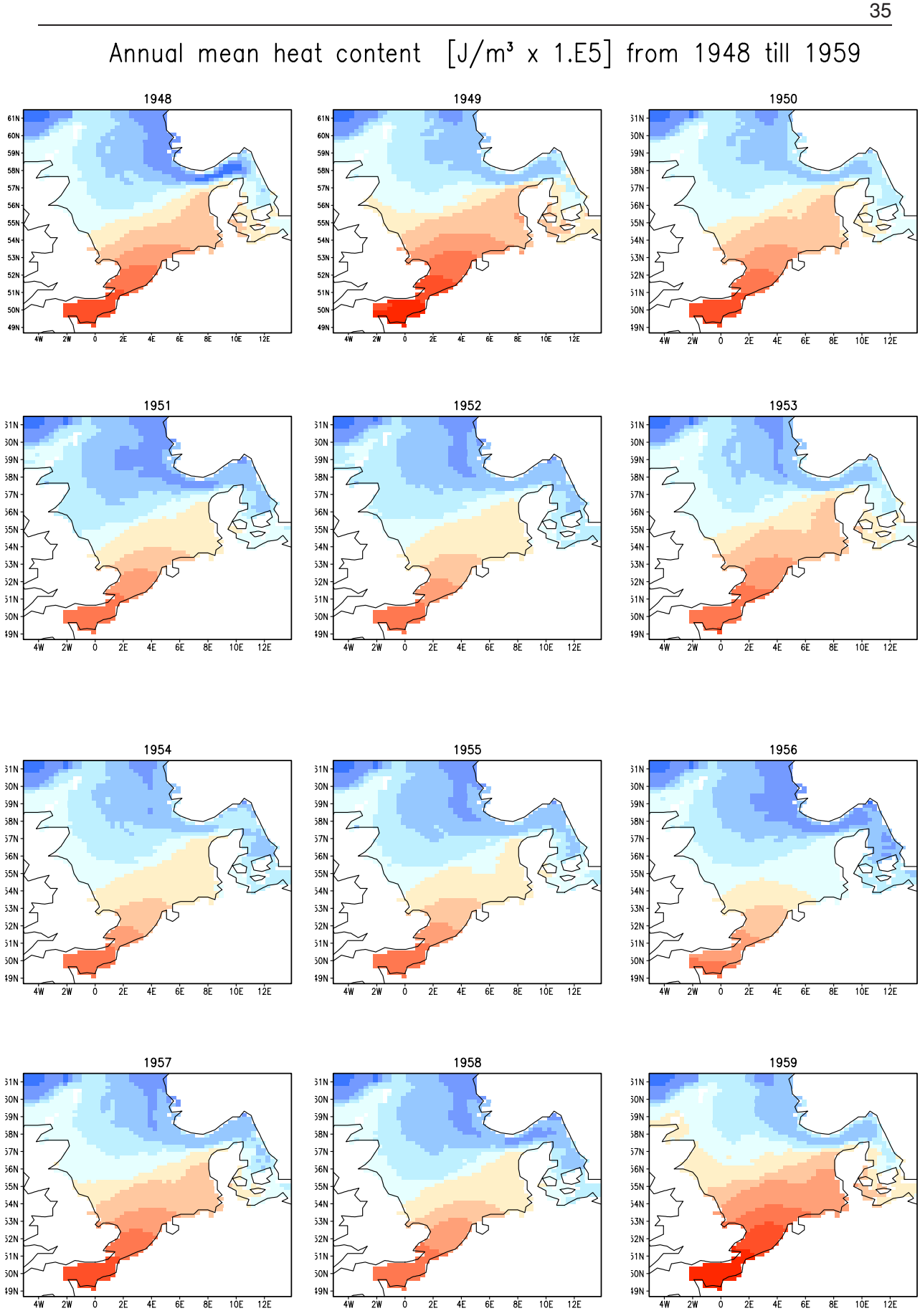

Figure C.1: *Mean annual heat content [10^5 J m^{-3}] from 1948 - 1959.*

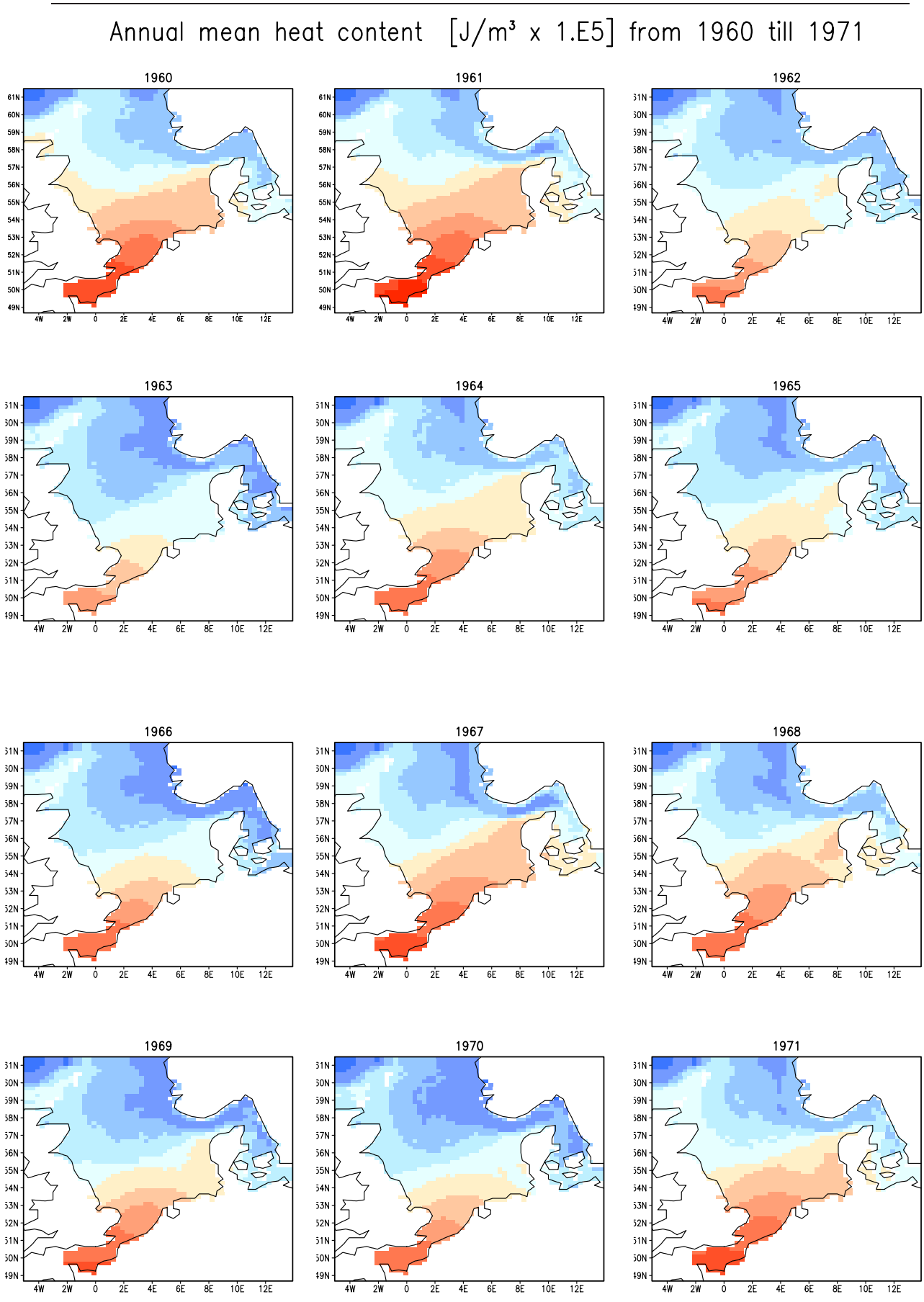

Figure C.2: *Mean annual heat content [10^5 J m^{-3}] from 1960 - 1971.*

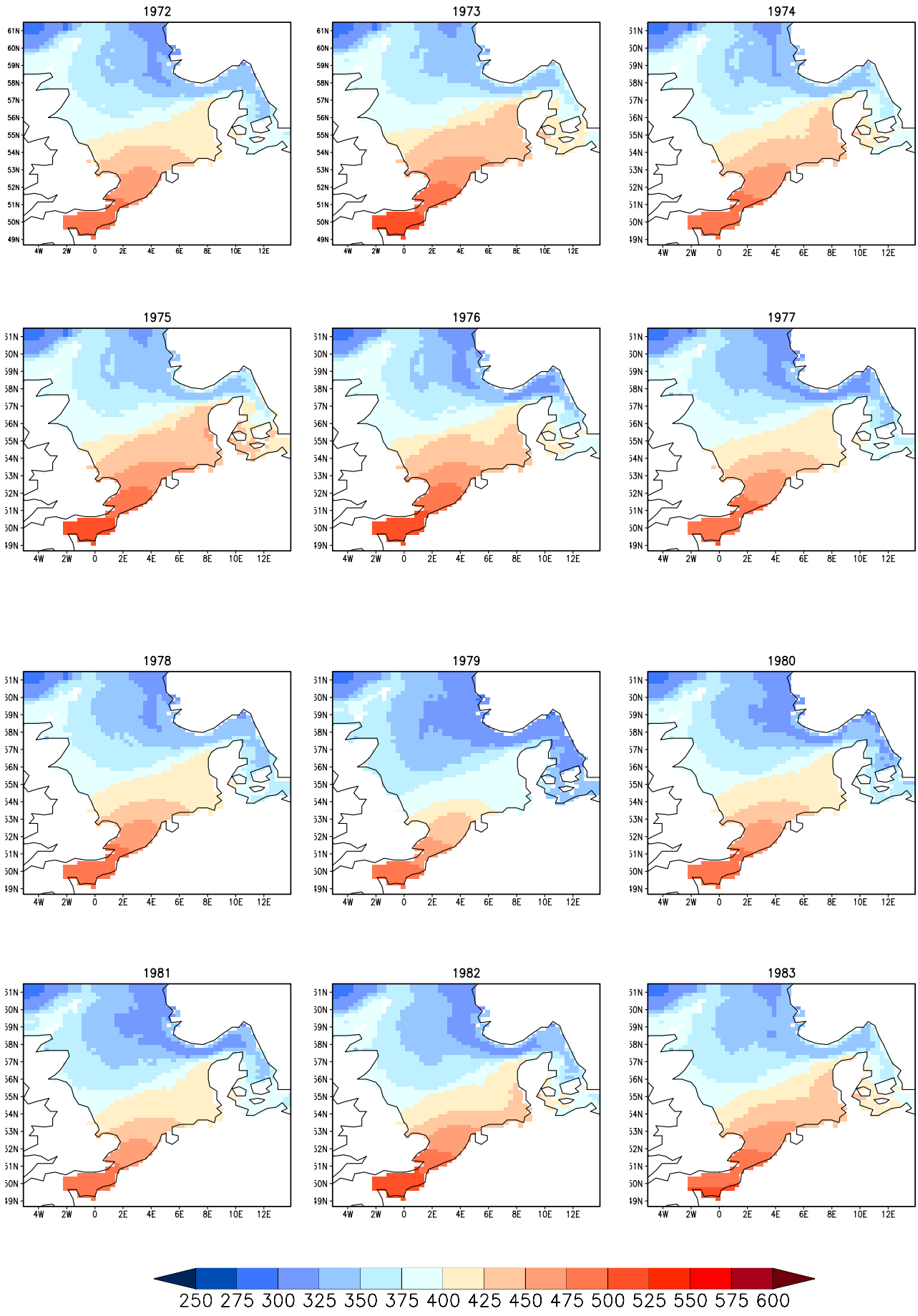

Figure C.3: *Mean annual heat content [10^5 J m^{-3}] from 1972 - 1983.*

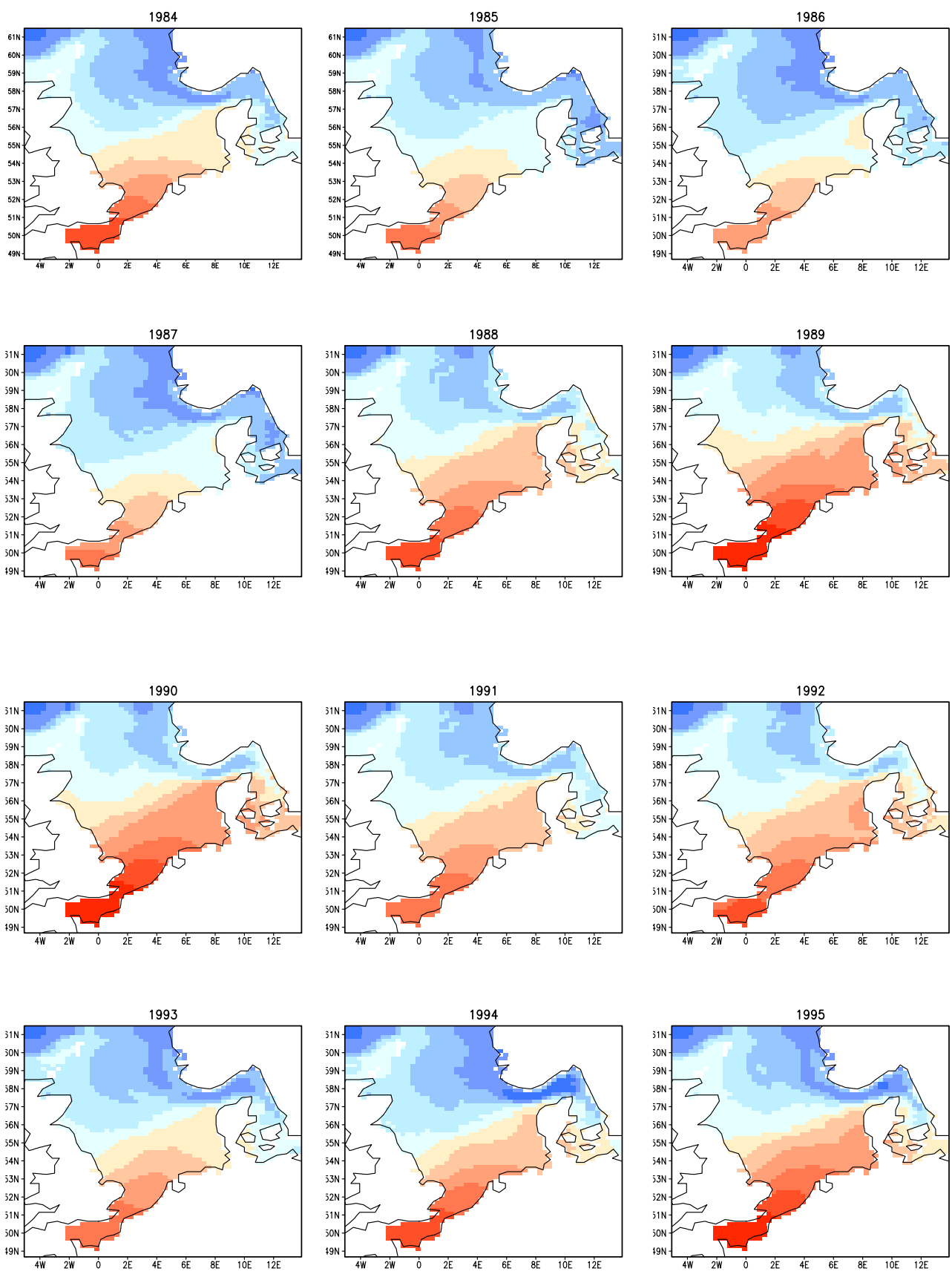

Figure C.4: *Mean annual heat content [10^5 J m^{-3}] from 1984 - 1995.*

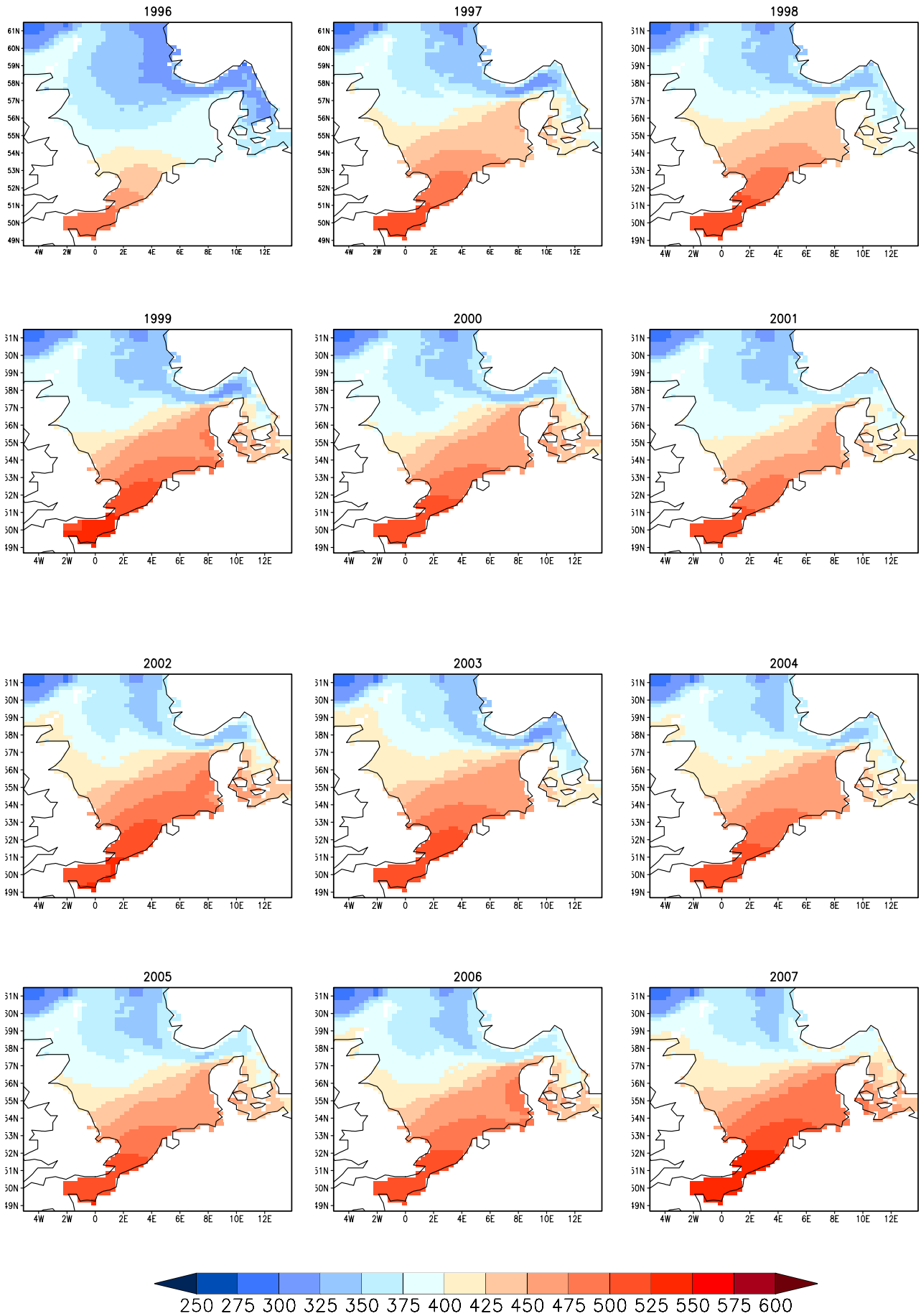

Figure C.5: *Mean annual heat content [10^5 J m^{-3}] from 1996 - 2007.*

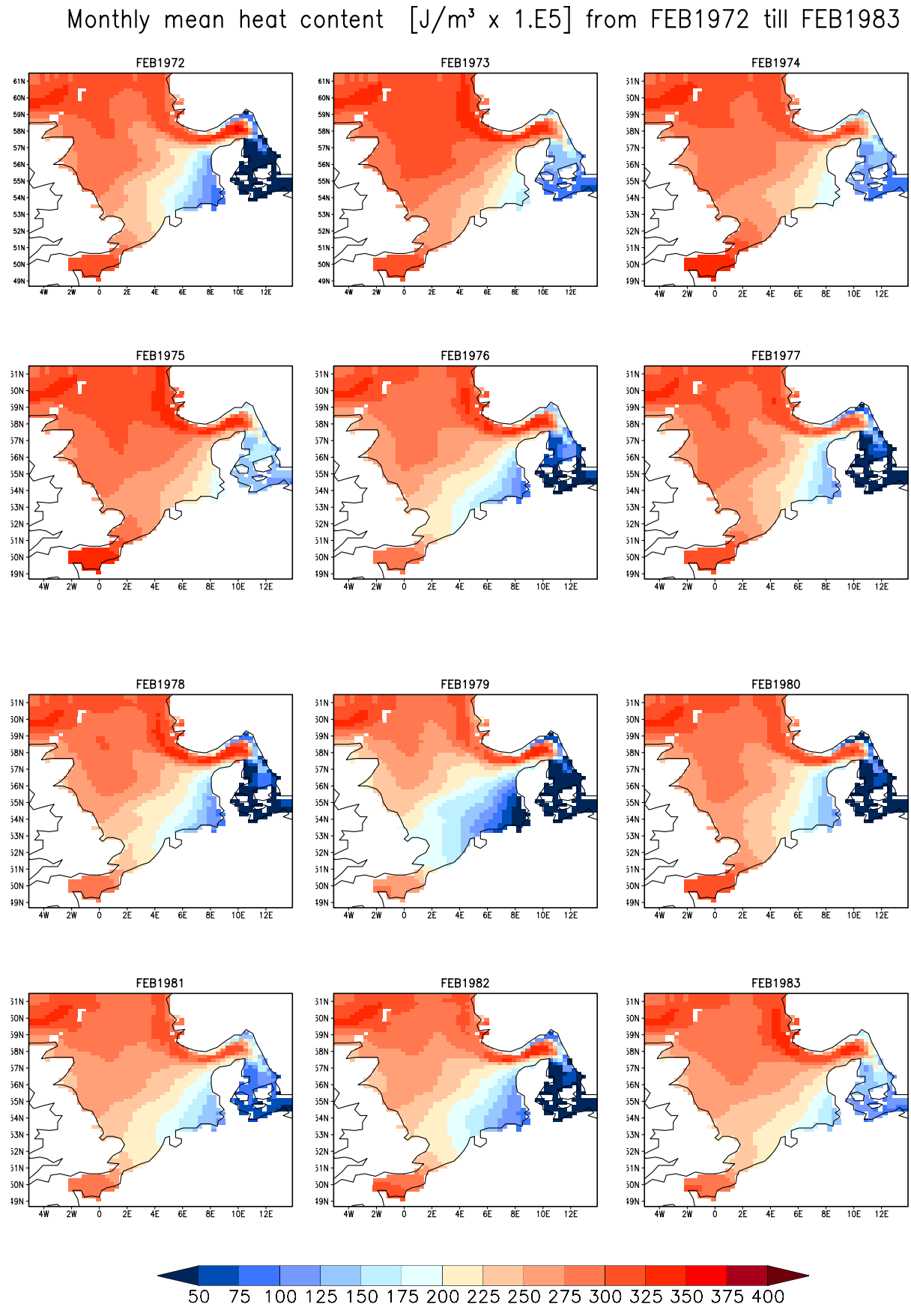

Figure C.6: *Mean heat content [10^5 J m^{-3}] for February from 1972 - 1983.*

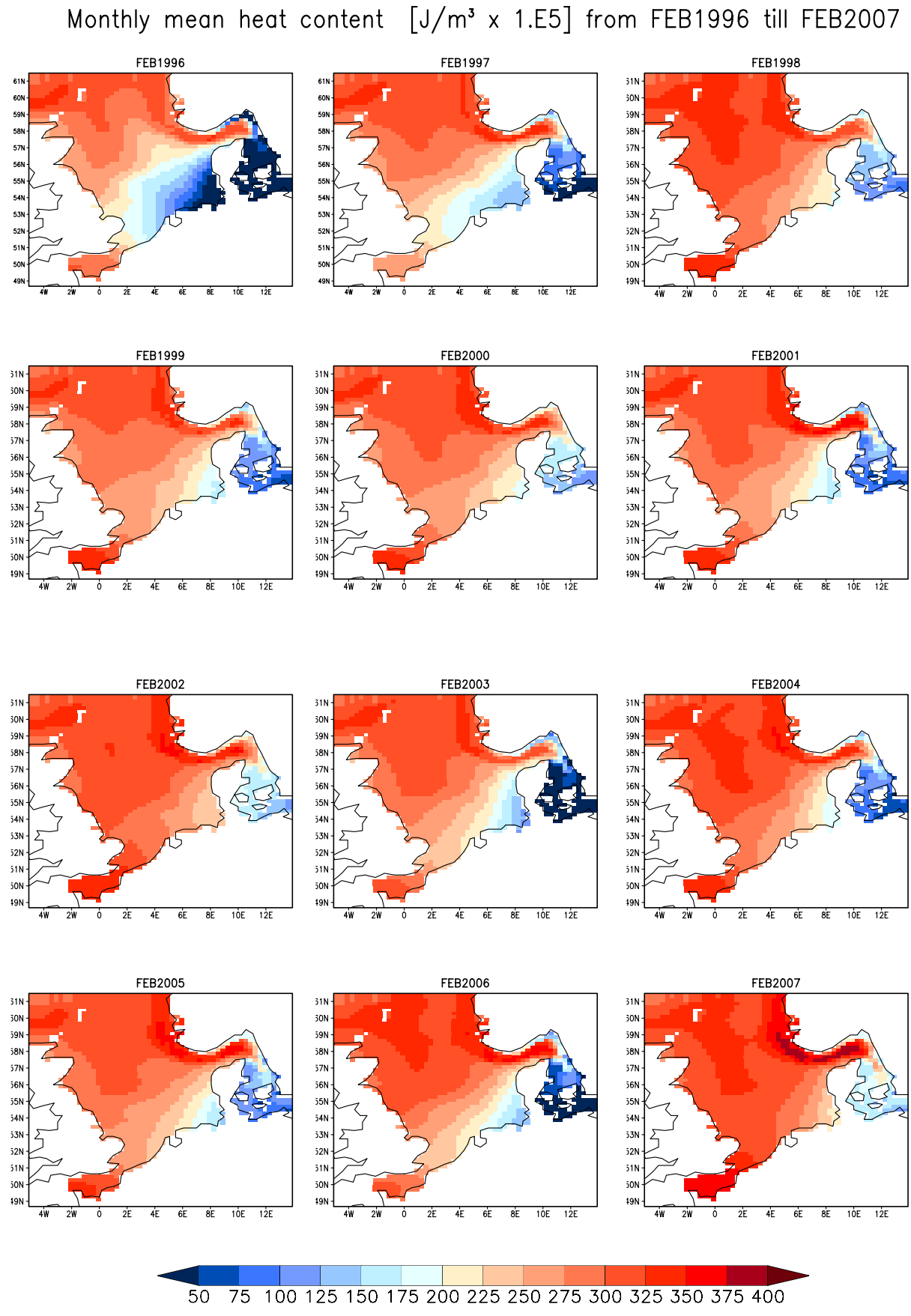

Figure C.7: *Mean heat content [10^5 J m^{-3}] for February from 1996 - 2007.*

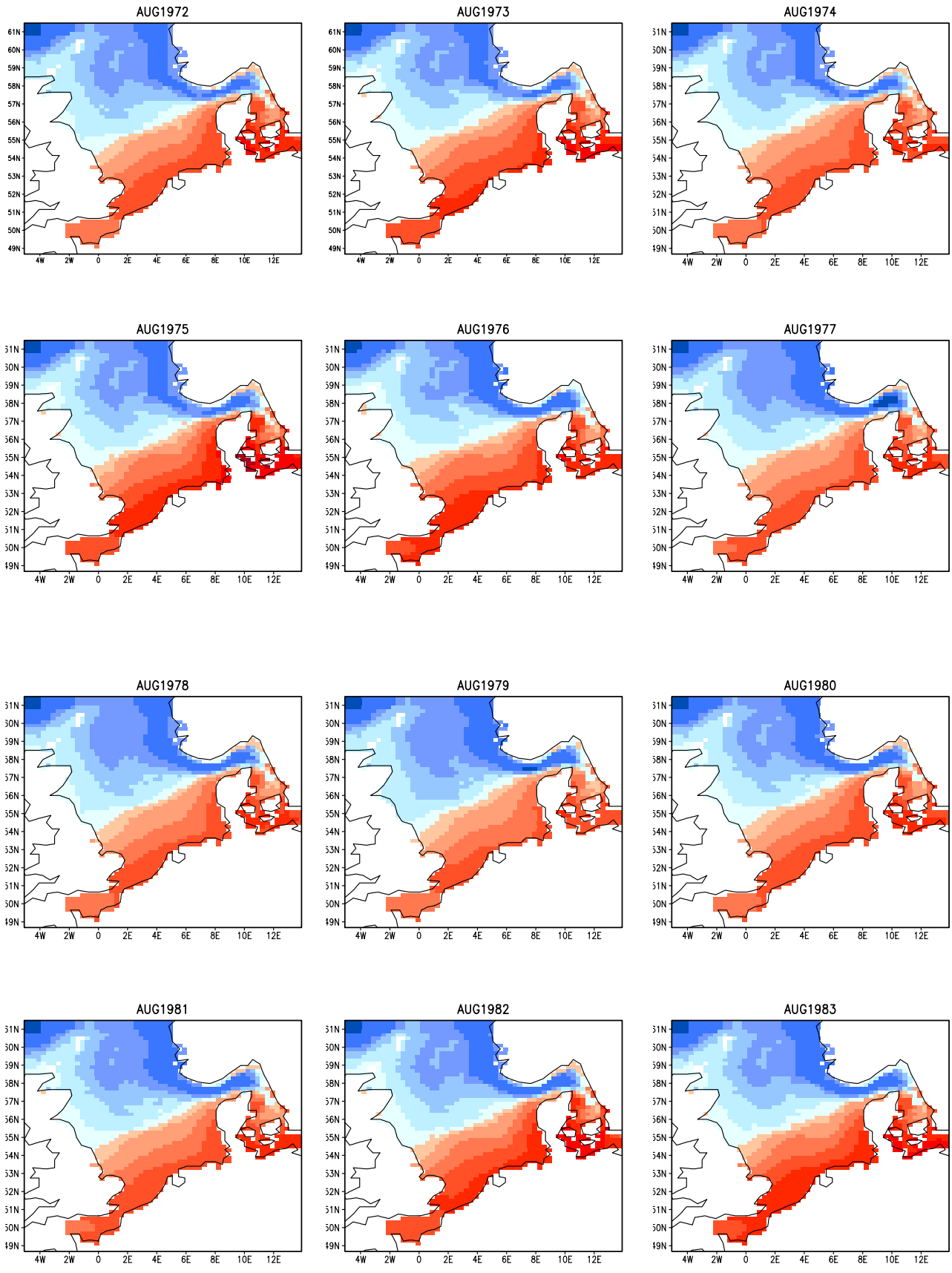

Figure C.8: *Mean heat content [10^5 J m^{-3}] for August from 1972 - 1983.*

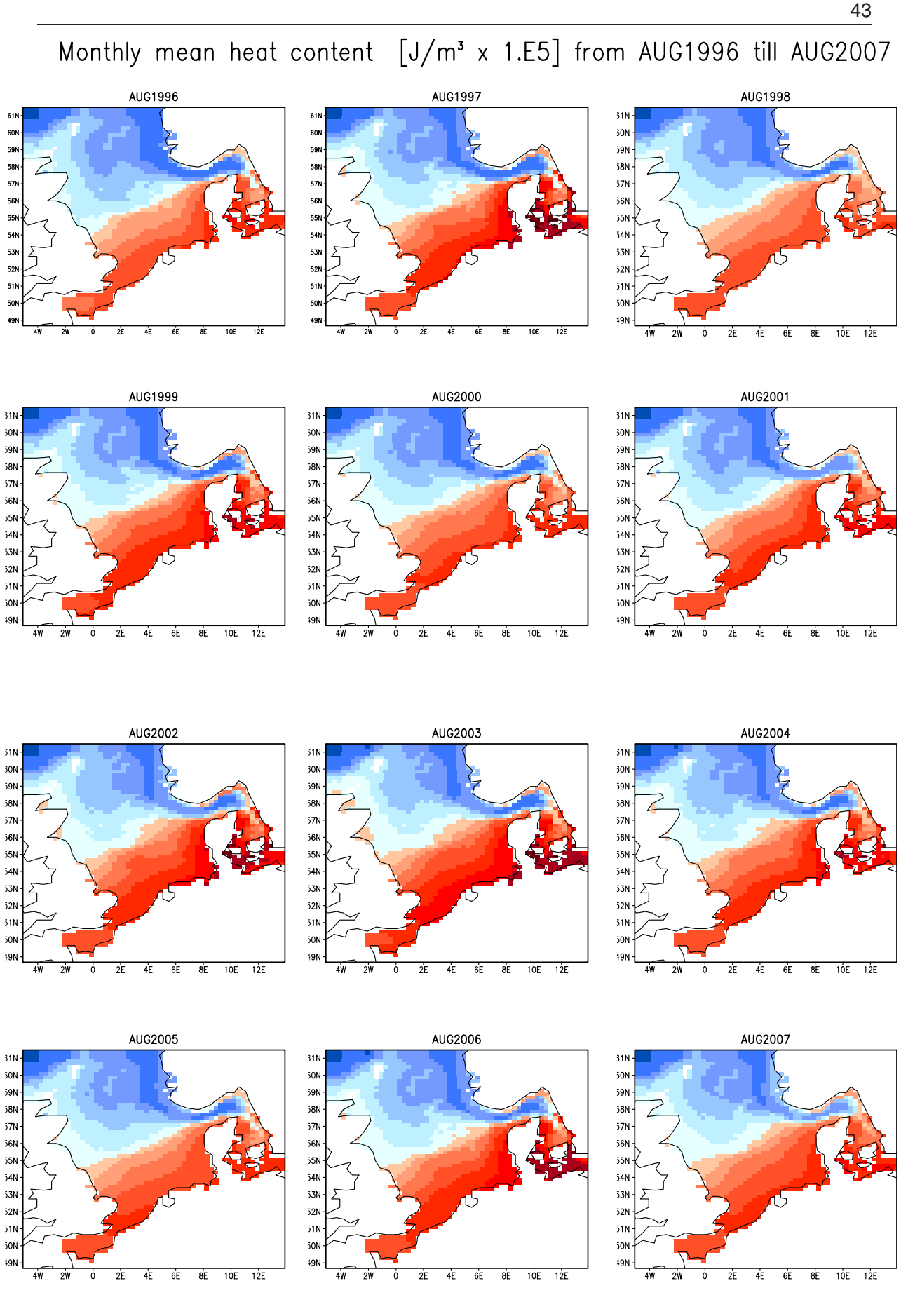

Figure C.9: *Mean heat content [10^5 J m^{-3}] for August from 1996 - 2007.*

List of Figures

List of Tables

Bibliography

Backhaus, J. O., 1985: A three-dimensional model for the simulation of shelf sea dynamics. *Deutsche Hydrographische Zeitschrift*, **38**, 165 – 187.

Backhaus, J. O. and D. Hainbucher, 1987: A finite difference general circulation model for shelf seas and its application to low frequency variability in the North-European shelf. In: J. Nihoul and B. Jamart, eds., *Three-Dimensional Models of Marine and Estuarine Dynamics*, pp. 221 –244. Elsevier Science Publishers, B.V. Amsterdam.

Becker, G. A., A. Frohse, and P. Damm, 1997: The Northwest European Shelf Temperature and Salinity Variability. *German Journal of Hydrography*, **49**(2/3), 135–151.

Becker, G. A. and M. Pauly, 1996: Sea surface temperature changes in the North Sea and their causes. *ICES Journal of Marine Science*, **53**, 887–898.

Bengtsson, L., S. Hagemann, and K. Hodges, 2004: Can climate trends be calculated from reanalysis data? *Journal of Geophysical Research*, **109**(D11), doi:10.1029/2004JD004536.

Burchard, H. and K. Bolding, 2001: GETM - a general estuarine transport model. Scientific documentation. Technical report, EUR 20253 EN, European Commision.

Charnock, H., K. Dyer, J. Huthnance, P. Liss, J. Simpson, and P. Tett, 1994: *Understanding the North Sea System*. Chapman & Hall. 222 pp.

Damm, P., 1989: Klimatologischer Atlas des Salzgehaltes, der Temperatur und der Dichte in der Nordsee, 1968 - 1985. Technical Report 89-6, Institut für Meereskunde, Hamburg.

Damm, P., 1997: Die saisonale Salzgehalts- und Frischwasserverteilung in der Nordsee und ihre Bilanzierung. Berichte aus dem ZMK - Reihe B: Ozeanographie 28, Institut für Meereskunde.

de Kok, J. M., C. de Valk, J. H. T. M. van Kester, E. de Goede, and R. E. Uittenbogaard, 2001: Salinity and Temperature Stratification in the Rhine Plume. *Estuarine, Coastal and Shelf Science*, **53**, 467–475. Doi:10.1006/ecss.2000.0627.

Delhez, É. J. M., P. Damm, E. de Goede, J. M. de Kok, F. Dumas, H. Gerritsen, J. E. Jones, J. Ozer, T. Pohlmann, P. S. Rasch, M. Skogen, and R. Proctor, 2004: Variability of shelf-seas hydrodynamic models: lessons from NOMADS2 Project. *Journal of Marine Systems*, **45**, 39–53.

Demirov, E. and N. Pinardi, 2002: Simulation of the Mediterranean Sea circulation from 1979 to 1993: Part I. The interannual variability. *Journal of Marine System*, **33-34**, 23–50.

Dippner, J. W., 1997: A note on SST anomalies in the North Sea in relation to the North Atlantic Oscillation and the potential influence on the theoretical spawning time of fish. *Ocean Dynamics*, **49**(2-3), 267–275.

Feistel, R., 1993: Equilibrium thermodynamics of seawater revisted. *Prog. Oceanog.*, **31**, 101 – 179.

Feser, F., R. Weisse, and H. von Storch, 2001: Multi-decadal atmospheric modeling for Europe yields multi-purpose data. *EOS Transactions*, **82**(28), pp. 305, 310.

Franke, H.-D., F. Buchholz, and K. H. Wiltshire, 2004: Ecological long-term research at Helgoland (German Bight, North Sea): retrospect and prospect - an introduction. *Helgoland marine research*, **58**(223-229).

Fung, I. Y., D. E. Harrison, and A. A. Lacis, 1984: On the variabbility of the net longwave radiation at the ocean surface. *Reviews of Geophysics and Space Physics*, **22**(2), 177–193.

Gordon, A. D. and J. L. McClean, 1999: Thermohaline Stratification of the Indonesian Seas: Model and Observations. *Journal of Physical Oceanography*, **29**, 198–216.

Holt, J. T., J. I. Allen, R. Proctor, and F. Gilbert, 2005: Error quantification of a high-resolution coupled hydrodynamic-ecosystem coastal-ocean model: Part 1 model overview and assessment of the hydrodynamics. *Journal of Marine Systems*, **57**, 167–188. Doi:10.1016/j.jmarsys.2005.04.008.

Holt, J. T. and I. D. James, 2001: An s coordinate density evolving model of the northwest European Continental Shelf, 1, Model description and density structure. *Journal of Geophysical Research*, **106**(C7), 14015–14034. DOI: 10.1029/2000JC000304.

Howarth, M., K. Dyer, I. Joint, D. Hydes, D. Purdie, H. Edmunds, J. Jones, R. Lowry, T. Moffat, A. Pomroy, and R. Proctor, 1994: Seasonal cycles and their spatial variability. In: H. Charnock, K. Dyer, J. Huthnance, P. Liss, J. Simpson, and P. Tett, eds., *Understanding the North Sea System*, pp. 5–25. Chapman & Hall.

Hurrell, J. W., 1995: Decadal trends in the North Atlantic oscillation: Regional temperatures and precipitation. *Science*, **269**, 676–679.

Janssen, F., 2002: *Statistische Analyse mehrjähriger Variabilität der Hydrographie in Nord- und Ostsee*. Ph.D. thesis, University of Hamburg.

Janssen, F., C. Schrum, and J. O. Backhaus, 1999: A climatological data set of temperature and salinity for the Baltic and the North Sea. *German Journal of Hydrography*. Supplement 9.

Jędrasik, J., W. Cieślikiewicz, M. Kowalewski, K. Bradtke, and A. Jankowski, 2008: 44 years hindcast of the sea level and circulation in the Baltic Sea. *Coastal Engineering*, **55**, 849–860. Doi:10.1016/j.coastaleng.2008.02.026.

Kalnay, E., M. Kanamitsu, R. Kistler, W. Collins, D. Deaven, L. Gandin, M. Iredell, S. Saha, G. White, J. Woollen, Y. Zhu, M. Chelliah, W. Ebisuzaki, W. Higgins, J. Janowiak, K. C. Mo, C. Ropelewski, J. Wang, A. Leetmaa, R. Reynolds, R. Jenne, and D. Joseph, 1996: The NCEP/NCAR 40-year reanalysis project. *Bulletin of the American Meteorological Society*, **77**(3), 437 – 471.

Karl, T., R. Quayle, and P. Groisman, 1993: Detecting climate variations and change: New challenges for observing and data management systems. *Journal of Climate*, **6**, 1481–1494.

Kauker, F., 1999: Regionalization of Climate Model Results for the North Sea. Report 99/E/6, GKSS.

Kondo, J., 1975: Air-sea bulk transfer coefficients in diabetic conditions. *Boundary-Layer Meteorology*, **9**, 91–112.

Levitus, S., 1982: Climatological Atlas of the World Ocean. Professional Paper 13, NOAA/ERL GFDL, Princeton, N.J. 173 pp.

Luyten, P. J., J. E. Jones, and R. Proctor, 2003: A Numerical Study of the Long- and Short-Term Temperature Variability and Thermal Circulation in the North Sea. *Journal of Physical Oceanography*, **33**(1), 37–56.

Luyten, P. J., J. E. Jones, R. Proctor, A. Tabor, P. Tett, and K. Wild-Allen, 1999: COHERENS – a coupled Hydrodynamical-Ecological Model for Regional and Shelf Seas: User documentation. Mumm report, Management Unit of the Mathematical Models of the North Sea.

Moll, A. and G. Radach, 1990: Zirkulation und Schadstoffumsatz in der Nordsee (ZISCH): ZISCH Parameter Report. Technical Report 1, Institut für Meereskunde.

O'Driscoll, K. T. A. and V. M. Kamenkovich, 2009: Dynamics of the Indonesian Seas circulation. Part II - The influence of bottom topography on temperature and salinity distributions. *Journal of Marine Research*. (submitted).

Omstedt, A. and D. Hansson, 2006: The Baltic Sea ocean climate system memory and response to changes in the water and heat balance components. *Continental Shelf Research*, **26**(2), 236–251. Doi:10.1016/j.csr.2005.11.003.

Orlanski, I., 1976: A simple boundary condition for unbounded hyperbolic flows. *Journal of computational physics*, **21**(3).

Pilar, P., C. G. Soares, and J. C. Carretero, 2008: 44-year wave hindcast for the North East Atlantic European Coast. *Coastal Engineering*, **55**, 861–871. Doi:10.1016/j.coastaleng.2008.02.027.

Pohlmann, T., 1996: Predicting the thermocline in a circulation model of the North Sea – Part I: model description, calibration and verification. *Continental Shelf Research*, **16**(2), 131–146.

Pohlmann, T., 2003: Eine Bewertung der hydro-thermodynamischen Nordseemodellierung. Berichte aus dem Zentrum für Meeres- und Klimaforschung; Reihe B Ozeanographie 46, Zentrum für Meeres- und Klimaforschung der Universität Hamburg, Institut für Meereskunde.

Pohlmann, T., 2006: A meso-scale model of the central and southern North Sea: Consequences of an improved resolution. *Continental Shelf Research*, **26**, 2367 – 2385.

Ratsimandresy, A. W., M. G. Sotillo, J. C. C. Albiach, E. Á. Fanjul, and H. Hajji, 2008: A 44-year high-resolution ocean and atmospheric hindcast for the Mediterranean Basin developed within the HIPOCAS Project. *Coastal Engineering*, **55**, 827–842. Doi:10.1016/j.coastaleng.2008.02.025.

Schrum, C. and J. O. Backhaus, 1999: Sensitivity of atmosphere-ocean heat exchange and heat content in the North Sea and the Baltic Sea. *Tellus*, **51 A**, 526–549.

Schrum, C., F. Siegismund, and M. St. John, 2003: Decadal variations in the stratification and circulation patterns of the North Sea. Are the 1990s unusual? In: *Hydrobiological Variability in the ICES Area, 1990 - 1999*, volume 219 of *ICES Marine Science Symposia*, pp. 121–131. Edingburgh.

Sebastião, P., C. G. Soares, and E. Alvarez, 2008: 44 years hindcast of sea level in the Atlantic Coast of Europe. *Coastal Engineering*, **55**, 843–848. Doi:10.1016/j.coastaleng.2008.02.022.

Siddorn, J. R., J. I. Allen, J. C. Blackford, F. J. Gilbert, J. T. Holt, M. W. Holt, J. P. Osborne, R. Proctor, and D. K. Mills, 2007: Modelling the hydrodynamics and ecosystem of the North-West European continental shelf for operational oceanography. *Journal of Marine Systems*, **65**, 417–219. Doi:10.1016/j.jmarsys.2006.01.018.

Siegismund, F. and C. Schrum, 2001: Decadel changes in the wind forcing over the North Sea. *Climate Research*, **18**, 39–45.

Skogen, M. D. and A. Moll, 2005: Importance of ocean circulation in ecological modeling: An example from the North Sea. *Journal of Marine Systems*, **57**, 289–300. Doi:10.1016/j.jmarsys.2005.06.002.

Skogen, M. D. and H. Søiland, 1998: A User's guide to NORWECOM v2.0 - The NORWegian ECOlogical Model System. Technical report, Institute of Marine Research; Division of Marine Environment, Bergen-Nordnes, Norway.

Sotillo, M., A. Ratsimandresy, J. Carretero, A. Bentamy, F. Valero, and F. González-Rouco, 2005: A high-resolution 44-year atmospheric hindcast for the Mediterranean Basin: contribution to the regional improvemnet of global reanalysis. *Climate Dynamics*, **25**, 219–236. DOI 10.1007/s00382-005-0030-7.

Tonani, M., N. Pinardi, S. Dobricic, and C. Fratianni, 2008: A high-resolution free-surface model of the Mediterranean Sea. *Ocean Science*, **4**, 1–14.

Umlauf, L. and H. Burchard, 2005: Second-order turbulence closure models for geophysical boundary layers. A review of recent work. *Continental Shelf Research*, **25**, 795–827. Doi:10.1016/j.csr.2004.08.004.

Uppala, P., S.M.and Kållberg, A. Simmons, U. Andrae, V. da Costa Bechtold, M. Fiorino, J. Gibson, J. Haseler, A. Hernandez, G. Kelly, X. Li, K. Onogi, S. Saarinen, N. Sokka, R. Allan, E. Andersson,

K. Arpe, M. Balmaseda, A. Beljaars, L. van de Berg, J. Bidlot, N. Bormann, S. Caires, F. Chevallier, A. Dethof, M. Dragosavac, M. Fisher, M. Fuentes, S. Hagemann, E. Hólm, B. Hoskins, L. Isaksen, P. Janssen, R. Jenne, A. McNally, J.-F. Mahfouf, J.-J. Morcrette, N. Rayner, R. Saunders, P. Simon, A. Sterl, K. Trenberth, A. Untch, D. Vasiljevic, P. Viterbo, and J. Woollen, 2005: The ERA-40 reanalysis. *Quart. J. R. Meteorol. Soc*, **131**, 2961–3012. Doi:10.1256/qj.04.176.

von Storch, H. and R. Weisse, 2008: Regional storm climate and related marine hazards in the Northeast Atlantic. In: H. Diaz and R.J.Murnane, eds., *Climate Extremes and Society*, pp. 54–73. Cambridge University Press. ISBN 978-0-521-87028-3.

Weisse, R. and H. Günther, 2007: Wave climate and long-term changes for the Southern North Sea obtained from a high-resolution hindcast 1958-2002. *Ocean Dynamics*, **57**, 161–172.

Wiltshire, K. H. and B. F. J. Manly, 2004: The warming trend at Helgoland Roads, North Sea: phytoplankton response. *Helgol. Mar. Res.*, **58**, 269–273.

Winther, N. G. and G. Evensen, 2006: A hybrid coordinate ocean model for shelf sea simulation. *Ocean Modelling*, **13**, 221–237. Doi:10.1016/j.ocemod.2006.01.004.